LINEARIZED MATHEMATICAL MODEL OF SATELLITE GROUND CONTROL STATION

BY

OGUNDELE, DANIEL AYANSOLA

(M.ENG./SEET/07/1665)

DEPARTMENT OF ELECTRICAL AND COMPUTER ENGINEERING,

SCHOOL OF ENGINEERING AND ENGINEERING TECHNOLOGY,

FEDERAL UNIVESITY OF TECHNOLOGY,

MINNA, NIGER STATE.

MARCH, 2010

LINEARIZED MATHEMATICAL MODEL OF SATELLITE GROUND CONTROL STATION

BY

OGUNDELE, DANIEL AYANSOLA

(M.ENG./SEET/07/1665)

A THESIS SUBMITTED TO

THE POST GRADUATE SCHOOL,

FEDERAL UNIVERSITY OF TECHNOLOGY,

MINNA, NIGER STATE.

IN PARTIAL FULFILMENT FOR THE REQUIREMENT FOR THE AWARD OF MASTER OF ENGINEERING (M.ENG.) DEGREE IN COMMUNICATION ENGINEERING.

MARCH, 2010

DECLARATION

I declare that this thesis "*Linearized Mathematical Model of Satellite Ground Control Station*" was done by me and has never been presented elsewhere for the award of a Master Degree. It is the result of my own research work except for works that have been cited in the References.

OGUNDELE, DANIEL AYANIOLA

(Name of Student)

09/04/2010

(Signature and date)

CERTIFICATION

This thesis titled: Linearized Mathematical Model of Satellite Ground Control Station by Ogundele, Daniel Ayansola (M.Eng/SEET/2007/1665) meets the regulations governing the award of the degree of Master of Engineering (M.Eng) of the Federal University of Technology, Minna and is approved for its contribution to scientific and literary presentation.

Engr. (Dr.) Y.A. Adediran
Supervisor

Signature & Date

Engr. A.G. Raji
Head of Department

Signature & Date

Prof. O. Usifo
Dean, SEET

Signature & Date

Prof. S.L Lamai
Dean, Postgraduate School

Signature & Date

DEDICATION

Dedicated to my beloved late mother, Olatorera Asande-Iji, for her insistence on me being educated and her encouragement when alive. To my family, who inspires and understands with me.

ACKNOWLEDGEMENTS

First of all my profound gratitude goes to God for the grace to successfully complete this work and for the gift of life.

I would like to express my profound gratitude and appreciation to my supervisor, Dr. Y.A. Adediran, for his guidance in the execution of this work, for keeping me on my toes and for his kind understanding. I am especially grateful for all the help he provided during the course of writing this thesis and his unalloyed support.

I would also like to thank the following people for their various contributions to the success of this work, the head of department Electrical and Computer Engineering Engr. A. G. Raji. The department's team of internal examiners Engr. J Kolo and Engr. C. Alenoghena, the team of project presentation assessors, for the advice and guidance given to me during the project presentation and the entire staff of the Electrical and Computer Engineering.

I would also like to acknowledge the Dean School of Engineering, Prof. O. Usifo for his support and the deputy Dean School of Engineering Dr. O. Chukwu for patiently proof reading the work.

I wish to extend my appreciation to the management and staff of the Federal University of Technology Minna as well as the management and staff of the National Agency for Space Research Development (NASDA) for the enabling environment given to me in the course of my studies.

Last, but not the least, I would like to thank my family for just being there, giving me the strength and the much needed moral support.

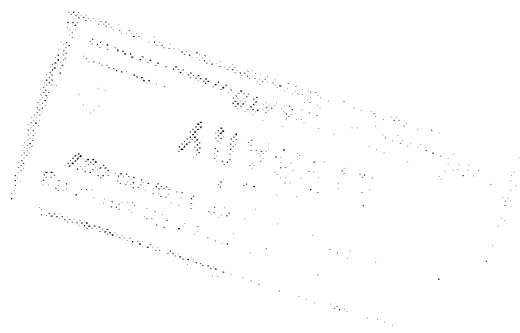

ABSTRACT

The current Satellite Ground Control Station is very complex and complicated. This, therefore, necessitated the need to develop a simplified model of Satellite Ground Control Station that will be easily understood by the operators of the system. The purpose of this thesis, Linearized Mathematical Model of Satellite Ground Control Station, is to develop mathematical models of the different components of a Satellite Ground Control Station, to linearize the models and to validate the models using computer assisted investigation so as to be sure that the model assumptions are valid and to establish confidence in the model. The behaviour of Satellite Ground Control Station models developed was described using qualitative and quantitative approaches. For the qualitative analysis, using linearization technique, the results obtained show that at the visible regions, $(0 \leq \gamma_1 \leq 1.4191\, rad)$ and $(4.8695 \leq \gamma_2 \leq 6.2840\, rad)$, the system is well linearized because the effects of noise and interference are minimal but at the invisible region, $(1.4191 < \gamma < 4.8695\, rad)$, the system was not well linearized due to the influence of noise and interference of signals. Individual components of the models were tested using quantitative analysis and the results obtained through the validation show that the calculated values were in conformity with the simulated values.

TABLE OF CONTENTS

CHAPTER FOUR

CHAPTER FIVE

LIST OF TABLES

LIST OF FIGURES

ABBREVIATIONS AND SYMBOLS

Abbreviations

ADC	Analog-to-Digital Converter
AGC	Automatic Gain Control
AHRS	Attitude and Heading Reference Sensor
AI	Artificial Intelligence
ASK	Amplitude Shift Keying
ATS	Automatic Targeting System
AOCS	Attitude and Orbit Control System
BER	Bit Error Rate
BPF	Band-pass Filter
CBERS	China-Brazil Earth Resources Satellites
CFR	Constant Hazard (or Failure) Rate
COMS	Communication, Ocean, and Meteorological Satellite
COTS	Commercial-off-the-Shelf
DBS – TV	Direct Broadcast Satellite Television
DFR	Decreasing Hazard (or Failure) Rate
EGSE	Electrical Ground Support Equipment
EIRP	Equivalent Isotropic Radiated Power
FM	Frequency Modulation
FSK	Frequency Shift Keying
FTA	Fault Tree Analysis

GCS	Ground Control Station
GEO	Geostationary Orbit
GPS	Global Positioning System
GSFC	NASA Goddard Space Flight Center
GSO	Geosynchronous Satellite Center
GSS2	Ground Station Software 2
GTDS GSFC's	Goddard Trajectory Determination SYstem
GUI	Graphical User Interface
HPA	High Power Amplifier
HST	High Speed Telemetry
HT	Hyper-Threading
IBBE	Integrated Baseband Equipment
IF	Intermediate Frequency
IFR	Increasing Hazard (or Failure) Rate
ITU	International Telecommunication Union
JStation	Java Satellite Ground Control Station
LEO	Low Earth Orbit
LNA	Low Noise Amplifier
MCC	Mission Control Center
MCS	Monitoring and Control Subsystem
MEO	Medium Earth Orbit
MW	Momentum Wheel
NASA	National Aeronautics and Space Administration

NASDA	National Space Development Agency of Japan
NCO	Numerical Control Oscillator
PM	Phase Modulation
PODS	Analytical Graphics' Precision Orbit Determination System
PSK	Phase Shift Keying
RF	Radio Frequency
RR	Radio Regulations
RW	Reaction WHeel
SBIR	Small Business Innovation Research
SCC	Satellite Control Center
SDR	Satellite Ground Station Software Defined Radio
SGCS	Satellite Ground Control Station
SSDL	Standford's Space System Development Laboratory
TCP/IP	Transmission Control Protocol/Internet Protocol
TC & R	Telemetry Command and Ranging
TFS	Time and Frequency Subsystem
TNC	Terminal Node Controller
TT & C	Telemetry Tracking and Command
UAS	Unmanned Aircraft System
UAV	Unmanned Aerial Vehicle
UTIAS/SFL	University of Toronto Institute for Aerospace Studies/ Space Flight
UTIAS/SFL	University of Toronto Institute for Aerospace Studies/Space Flight

	Laboratory
UWE-1	University of Würzburg's Experimental Satellite

Symbols

A_0	Quantizing amplitude of local carrier signature
A_z	Azimuth angle
d	distance from satellite to ground station (m)
$d_1 and\ d_2$	Distance from the earth station to the satellite
D	caliber size (diameter) of the satellite receiving antenna (m)
f_v	Max. video frequency (Hz)
F	Deaccentuation improving factor
$g(t)$	Waveform of the modulated signal's envelope
G_r	Gain of the receiver
G_t	Gain of the transmitter
IF_Σ	IF sum signal
IF_Δ	IF difference signal
k_{p1}	Modulation index of telemetry sub-carrier
k_{p2}	Modulation index of ranging sub-carrier
l_e	Longitude of the Earth station
l_s	Longitude of the subsatellite point
L_a	Attenuation in atmosphere
L_e	Latitude of the Earth station

L_p	Path Loss
L_{ra}	Losses associated with receiving antenna
L_s	Longitude of the sub-satellite point
L_{ta}	Losses associated with transmitting antenna
$m_1(t)$	Telemetry sub-carrier signal,
$m_2(t)$	Ranging tone sub-carrier
pitch	Rotation about the Y_B axis
P_r	Received power
P_t	Transmitted power
$P_t G_t$	Effective isotropic radiated power (EIRP)
roll	Rotation about the X_B axis
r_e	Vector from the center of the earth to the Earth station
r_s	Vector from the center of the earth to the satellite
R_0	Distance between the satellite ground control station and object
R_1	Distance between the satellite and satellite ground control station
$s(t)$	Input Phase Modulated (PM) signal
S/N	Video signal to noise ratio (dB)
T_a	Antenna noise temperature
T_r	HF tuner noise temperature
T_s	Period
ω_1	Center frequency of the carrier wave
ω_c	Angular Frequency

X_B	Axis tangent to the orbital plane and lies in the orbital plane
yaw	Rotation about the Z_B axi
Y_B	Axis perpendicular to the orbital plane
Z_B	Axis directed towards the center of the earth
η	Antenna efficiency, usually is taken as 0.65 in engineering.
Δf_v	Video frequency deviation (Hz)
ΔL	Down-going additional loss (dB)
$\Delta\varphi$	Phase delay
$\Delta\emptyset$	Phase offset information between sum and error channel
$\gamma_1 and\ \gamma_2$	Angles between re and rs the satellite
θ_1	Initial phase of the carrier
φ_k	Carrier's phase of the data k
λ_1	Wavelength

LINEARIZED MATHEMATICAL MODEL OF SATALLITE GROUND CONTROL STATION

BY

OGUNDELE, DANIEL AYANSOLA

(M.ENG./SEET/07/1665)

DEPARTMENT OF ELECTRICAL AND COMPUTER ENGINEERING,

SCHOOL OF ENGINEERING AND ENGINEERING TECHNOLOGY,

FEDERAL UNIVESITY OF TECHNOLOGY,

MINNA, NIGER STATE.

MARCH, 2010

CHAPTER ONE

1.0 INTRODUCTION

1.1 Satellite Communications System

In astronomical terms, a satellite is a celestial body that orbits around a planet such as the moon which is a natural satellite of the Earth. In aerospace terms, however, a satellite is a space vehicle launched by humans and orbits the Earth or another celestial body (Wayne, 2001). The main purpose of a satellite is to carry the communications payload which provides revenue-earning services to the customers in a reliable and timely fashion (Evans, 1999).

"Satellite communications" refers to communication systems that employ communications satellite as a relay station. Communications satellites are man-made satellites that orbit the Earth, providing a multitude of communication functions to a wide variety of consumers including military, governmental, private, and commercial subscribers. It is a microwave repeater in the sky that consists of a diverse combination of one or more of the following: receiver, transmitter, amplifier, regenerator, filter, on-board computer, multiplexer, demultiplexer, antenna, and waveguide (Wayne, 2001). Geostationary Earth Orbit, GEO, satellites are the backbone of the commercial satellite communications industry. Large GEO satellites can serve one-third of the earth's surface, and can carry up to 4 Gbps of data, or transmit up to 16 high power direct broadcast satellite television (DBS-TV) signals, each of which can deliver several video channels (Timothy *et al.*, 2003).

The origin of satellite communications can be traced to an article written by Arthur C. Clarke in the British radio magazine "*Wireless World*" in 1945. Clarke suggested that a radio relay satellite in an equatorial orbit with a period of 24 hours would remain stationary with respect to the earth`s surface and make possible long-distance radio links. He stated further that three of such relay stations at 120^{0} apart will cover the whole world. At that time, Clarke was serving in the British Royal Air Force, and was interested in long distance radio communications (Timothy *et al* , 2003).

1.1.1 Satellite Orbits

Satellites which orbit the earth follow the same laws that govern the motion of the planets around the sun (Dennis, 2002). There is a large range of satellite orbits, but not all of them are of use for satellite communications. Those most used are low earth orbit (LEO), geostationary orbit, Tundra orbit, Molnya orbit, and inclined circular geosynchronous orbit. The 24-hour geostationary (circular) orbit with an altitude of 35,786 km is the most commonly used for fixed communications. This orbit imposes minimal tracking constraints on the earth stations; it is only the perturbations of the orbit caused by the gravitational forces of the stars and planets and non-sphericity of the Earth which require tracking. However, for Earth stations located at extreme latitudes, the elevation angle becomes very small and this causes propagation problems associated with the longer path in the troposphere. In the extreme, at the polar caps, the geostationary (circular) orbit is not visible. Thus for systems that require coverage of these regions highly eccentric, elliptical orbits inclined at 63.4^{0} to the equatorial plane exhibit significant apsidal dwells around their apogee. The two types of orbits in this category are Molnya orbit and the

Tundra orbit. The Molnya orbit was first used by the Soviet Union in the 1960s for television transmission to its remote areas, it has an apogee of around 40,000 km and a perigee of around 1,000 km. Similar characteristics are exhibited by the second, the Tundra orbit, which has an apogee of 46,300 km and a perigee of 25,250 km. Both orbits are used for land mobile satellite systems and for complementing the geostationary orbit in achieving worldwide coverage (Evans, 1999).

Low earth circular orbits (at altitudes of 500-1500 km) are being used for earth resources, data relay and navigation satellites as well as low-cost store-and-forward communications systems. In recent years, the use of low earth orbits at around 1,000 km altitudes has increased owing to their ability to provide global coverage for mobile and personal communications users. Two examples are the Iridium system with 66 satellites and Globalstar system of 48 satellites (Timothy *et al*., 2003). Low Earth Orbiting satellites are visible for only a period of time from the point of view of an observer on earth. They can dump data to the Ground Station when they passby a Ground Station area (Yu, 2005).

1.1.2 Basic Elements of Satellite Communications System

A satellite communications system is made up of two basic elements namely: space segment and ground segment as shown in Figure 1.1. The space segment consists of the satellites plus control or telemetry, and tracking and command (TT & C) stations to maintain the satellites in orbit (Evans, 1999). For a GEO operational system to be considered secure the operational satellite is backed up by an in-orbit spare satellite as well as, in some cases, a ground spare ready for launch in case of malfunction of either of

the orbiting satellites. The TT & C station is necessary to keep the satellites operating in space (Timothy *et al.*, 2003).

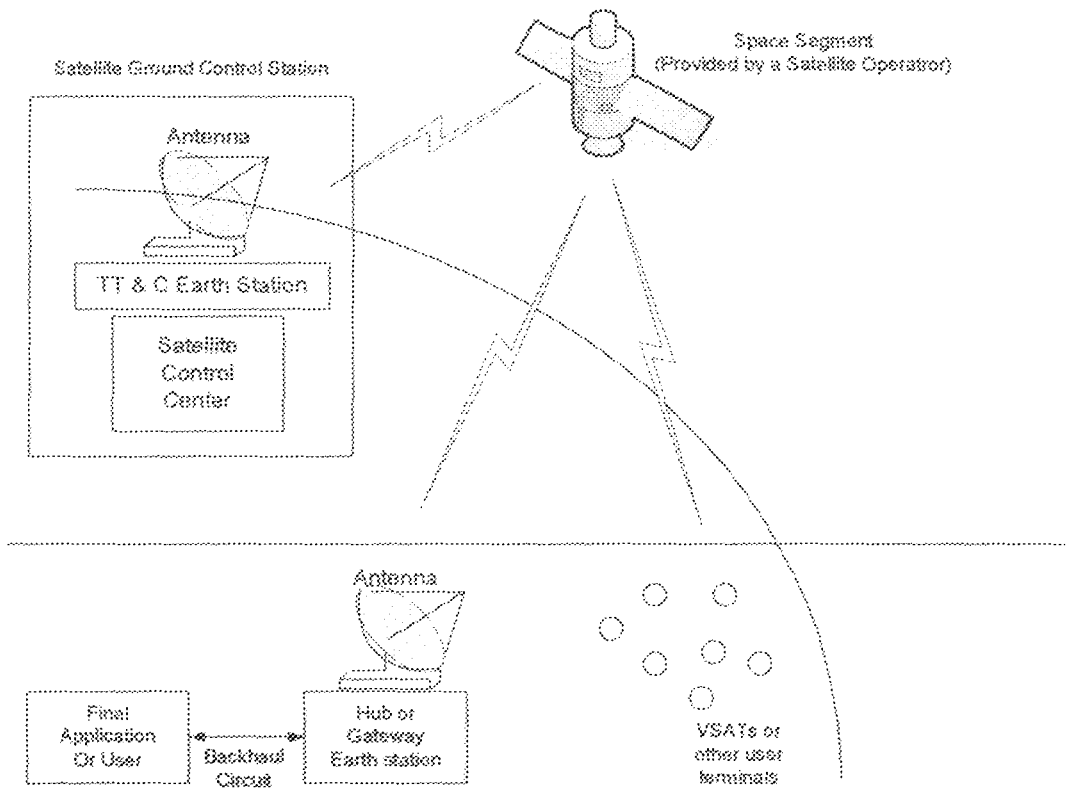

Fig. 1.1: Basic Elements of Satellite Communications System

The satellites are made up of two major components namely, communications payload and spacecraft bus. The communications payload consists of the satellite antennas plus the repeater. The spacecraft bus contains the house-keeping systems to support the payload and consists of Spacecraft structure, Electrical power subsystem, Propulsion susbsystem, Attitude and Orbit Control Subsystem and Thermal control subsystem.

The ground segment of the satellite system consists of all of the communicating earth stations which access the operational satellite. The ground station's job is two-fold. In the case of an uplink or transmitting station, terrestrial data in the form of baseband signals is passed through a baseband processor, an up-converter, a high-powered amplifier, and through a parabolic dish antenna up to an orbiting satellite. In the case of a downlink, or receiving station, the ground station works in the reverse fashion as the uplink, ultimately converting signals received through the parabolic antenna to baseband signal.

1.2 Satellite Ground Control Station (GCS)

Satellite Ground Control Station is the hub of a satellite communications system or an unmanned aircraft system (Philip, 2002). It supports the space segment and relays to users mission data generated by onboard instruments and received from the spacecraft. It consists of ground station and control centre working together to support the spacecraft and the data user (James and Wiley, 1999). The ground station performs like a communication bridge between the satellites and the ground, sending the commands to satellites as the ground centre requests and receiving the telemetry feedback data from satellites when they pass by the ground station horizon (Evans, 1999).

1.2.1 Basic Functions of Satellite Ground Control Station

A satellite ground control station performs its functions in order to maintain the state of health and mission readiness of an on-orbit satellite. These functions include: station keeping operations, orbit determination and maintenance, telemetry processing and commanding (Scott and John, 1993).

(a) Station Keeping Operations

Station keeping is a minor maneuver that a satellite in geostationary orbit (GEO) or low Earth orbit (LEO) must make over its mission life to compensate for orbital perturbations (Timothy *et al.*, 2003). In addition to having its attitude controlled, it is important that a geostationary satellite be kept in its correct orbital slot (Dennis, 2002).

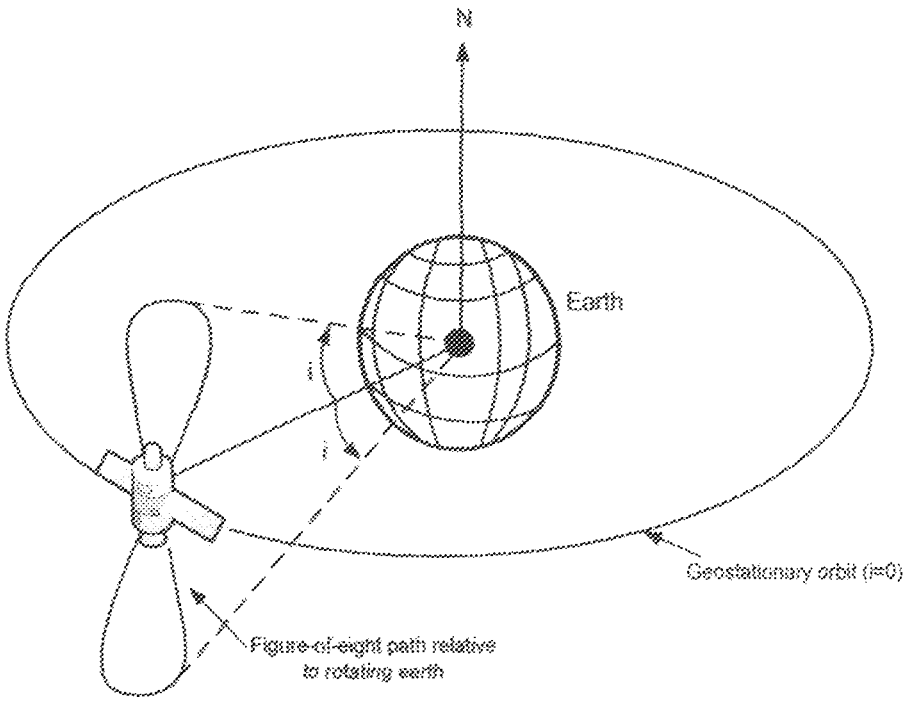

Fig. 1.2 Satellite in Geosynchronous orbit of non-zero inclination

Station keeping operations involve orbit control, technological status monitoring and attitude control. For geostationary and highly-eccentric orbits, the sun and moon affect the inclination and ascending node of the orbit (Evans, 1999), if uncorrected, this perturbation would increase an initially zero inclination to around 15^{0} before again reducing to zero over a period of 54 years. Therefore,

there is need to keep the inclination to zero (Timothy *et al.*, 2003). A geostationary orbit with a non-zero inclination describes a figure-of-eight path with respect to the rotating earth, as shown in Fig 1.2 (Evans, 1999).

(b) Orbit Determination and Maintenance

Orbit determination and maintenance is the ability to determine, predict and maintain the orbit of a satellite around the earth. To calculate the orbit of each satellite the ground station must reference it from a known position in space, the center of the earth. The fundamental coordinate system, to which spacecraft motion is referred, is generally the inertial frame which is fixed with respect to the stars. The ground control facility needs to accurately determine a satellite's position in order to acquire and downlink data (Scott and John, 1993). The orbit determination problem is the problem of finding the parameters that determine the satellite's position and velocity in space at a specified time (Darrel *et al.*, 2001).

(c) Telemetry Processing

Telemetry is the remote measurement and collection of data from a satellite. This data is the only means of accurately determining the state of a satellite (Xu, 2005). Common elements of telemetry data include: subsystem status data, payload cconfigurations and operations data, sensors data (e.g., star sensors or gyroscopes), and command response data. Extensive real time processing is required to quickly isolate and analyze telemetry data in order to have it available for the ground control system to use (Scott and John, 1993).

(d) Commanding

In order to transmit commands to a satellite it is essential that a stable ground-to-space link is established that minimizes environmental transmission losses. This link is established when a satellite ground control station can track satellite. An autotrack can be employed in which satellite ground control station will track the satellite automatically without operator's interaction. Once a link has been established commands can be transmitted from the ground control station to the satellite. In response to the commands sent, the satellite will transmit telemetry back to the ground control station (Scott and John, 1993).

1.2.2 Organization of Satellite Ground Control Station

Fig 1.3 shows the block diagram of satellite ground control station. It consists of the following main subsystems: Antenna Subsystem, RF Subsystem, Integrated Baseband Equipment Subsystem (IBBE), Time and Frequency Subsystem (TFS), Monitor and Control Subsystem (MCS) and Satellite Control Center (SCC).

(a) Antenna Subsystem

The dramatic increase in satellite communications capacity, capability and flexibility over the last decade has been made possible by improvements in techniques and in the design of components both in the space and ground segments. A key factor in achieving these improvements has been advances made in antenna technology. The antenna provides the vital link between the ground and the satellite, performing such complex operations as: simultaneous reception and transmission of communication signals, rejection of interference from neighbouring

systems both space and terrestrial, and maintaining of accurate pointing between earth station and satellite (Lu *et al.*, 2005).

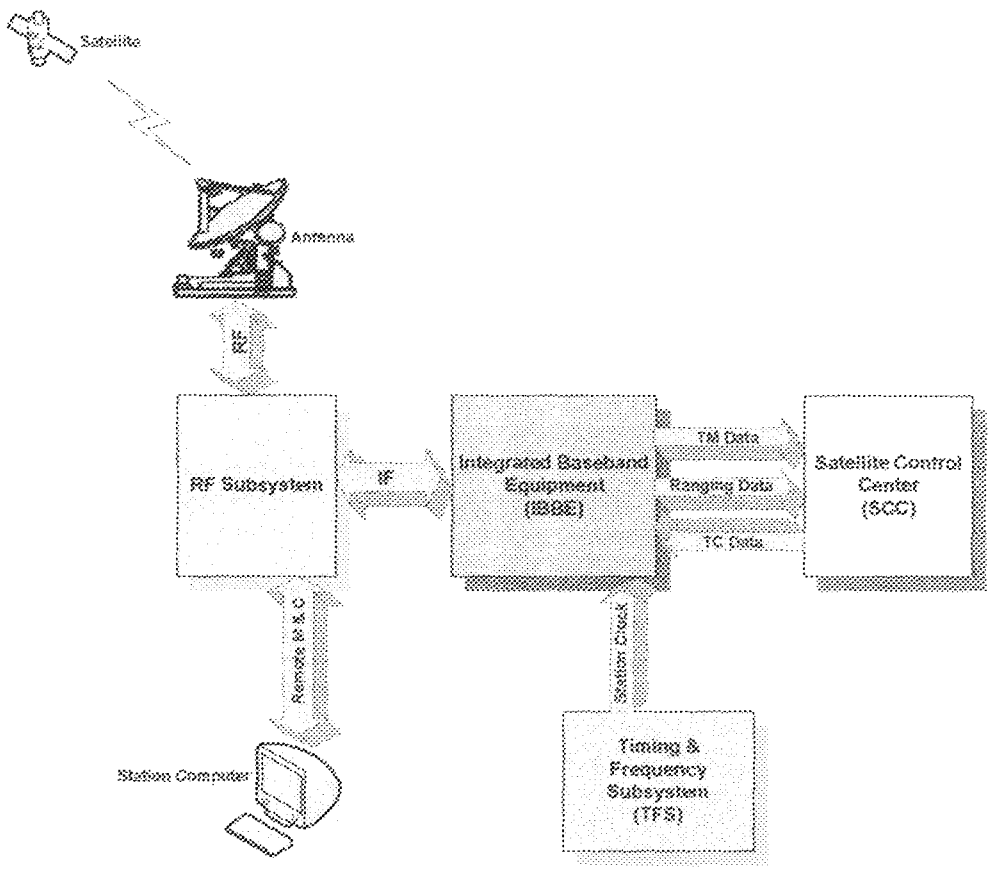

Fig. 1.3: Block diagram of a Satellite Ground Control Station

(b) RF Subsystem

Frequencies that are high enough to be efficiently radiated by an antenna and propagated through free space are commonly called radio frequencies, or simply RFs. In the modulator, the information acts on or modulates the RF carrier producing a modulated waveform. The radio-frequency subsystem contains the following: On the receiving side, the RF subsystem contains low noise amplifying equipment for routing the received carriers to the demodulating channels. The

transmitting side contains equipment for coupling the transmitted carriers and power amplifiers (Shulin, 2005).

(c) **Integrated Baseband Equipment (IBBE) Subsystem**

Baseband describes modulating (intelligence) signal in a communications system. Integrated Baseband Equipment (IBBE) is the central component of Telemetry Tracking and Command (TT & C) Ground Station; it is the functional and flexible glue, that is, interface between the Satellite Control Center (SCC) and the station RF section to allow telemetry reception, satellite telecommand transmission and satellite ranging (distance measurement) (Xu, 2005).

(d) **Time and Frequency Subsystem (TFS)**

A stable and reliable timing system is indispensable to satellite tracking and communication system so as to be able to carry out its activities correctly. TFS is an important part of the satellite tracking and communication system. It synchronizes the time of all the equipment in ground station (Wang, 2005).

(e) **Monitoring and Control Subsystem (MCS)**

MCS monitors and displays the following information of ground station equipment: operation mode, operation parameter, equipment configurations and equipment status. It monitors the failure of equipment and gives out alarm in case of failure. MCS system can automatically switch-over between the online and the stand-by equipment, and notify the operators for those equipment with redundancy. MCS supports remote control from Satellite Control Center, sends control to equipment, and reports the state of TTC equipment (Ju, 2005).

(f) Satellite Control Centre (SCC)

Satellite Control Centre is the ground operation decision centre of any satellite mission. Its main function is to ensure that the satellite performance is kept high right away from its injection up to the end of its life. SCC is used for telemetry (TM) data analysis as well as the telecommand (TC) generation, for the execution of the satellite orbit's attitude determination and prediction and for the generation of commands for the orbit and attitude manoeuvres of the satellite (Huiping, 2005).

1.2.3 Telemetry, Tracking and Command (TT & C)

Telemetry, tracking and command (TT & C) subsystem provides vital communication to and from the spacecraft. It is the only way through which we can observe and control the spacecraft's function and condition from the ground (Timothy *et al.*, 2003). The main activities of the TT & C are discussed hereunder.

(a) Telemetry:

Telemetry consists of measurements of the health of the satellite taken by sensors and transmitted to a ground monitoring station. There are two basic categories of telemetry: Health and Status, and Payload Data. A ground monitoring station receives and relays the telemetry to the satellite control facility where it is used to determine the operational status of the satellite and its subsystems. TT & C locks to the downlink carrier, demodulates the subcarrier and symbol, decodes and frame-synchronizes the bits.

(b) Commanding:

Commanding is the act of controlling a satellite. Commanding of a satellite is accomplished by sending to it signals which initiate an action or change the configuration in some way. Commands may be executed by the satellite immediately upon receipt or stored for later execution. Some commands are part of onboard software that allows the satellite to execute certain functions autonomously when a predefined condition exists. Commands may direct the thrusters to fire to change the orbit or may reconfigure the payload to meet the needs of users.

(c) Tracking:

Tracking involves determining a satellite's position, altitude and other orbital parameters. Many satellites carry a beacon which transmits a signal to help ground tracking receivers locate the satellite. On-board sensors, such as star trackers, horizon scanners and inertial navigation sensors provide other tracking data. Tracking information is essential to determine a satellite's orbital parameters so that an accurate prediction can be made of where the satellite will be in the future. In this way, the satellite's orbit can be adjusted so that it will be where it is supposed to be when it is supposed to be. To attain the accuracy that is needed usually requires relatively large antennas; therefore, the monitoring stations are normally fixed sites.

1.4 Statement of the Problem

From the analysis of the current Satellite Ground Control Station it was discovered that there were no mathematical details of each of its components and their linearization. As a result of this the operators could not have a thorough understanding of the system, thereby, necessitating the need for modelling and linearization of Satellite Ground Control Station. In addition, there is also need for the validation of the model in order to be ascertained that the system modelled conforms with the assumptions made and accomplishes the intended results. For the in-depth understanding of the system, the results of the research carried out on the modelling and linearization of Satellite Ground Control Station are presented in this thesis.

1.5 Objectives of the Thesis

The main objectives of this thesis are as follows:

a) To develop a mathematical model of Satellite Ground Control Station.

b) To linearize the model of Satellite Ground Control Station developed against noise and interference.

c) To validate the model of Satellite Ground Control Station developed.

1.6 Project Methodology

1.6.1 Modelling

A model is a pattern, plan, representation, or description designed to show the structure or workings of an object, system, or concept. It is a description of observed behaviour,

simplified by ignoring certain details. Models allow complex systems to be understood and their behaviour predicted within the scope of the model. The models of Satellite Ground Control Station proposed will enable the operators to understand the mathematical representation of each of its components.

1.6.2 Model Linearization

A linearized model is an approximation to a non-linear system, which is valid in a small region around the operating point of the system. The approximation is based on the derivatives of the system. These derivatives are evaluated at the operating point of the model which includes the values of inputs and states within the model. Engineers often use linearization in the design and analysis of control systems and physical models. In this thesis, every block of the Satellite Ground Control Station models was individualy linearized in order to determine the effects of noise and interference on the system.

1.6.3 Model Validation

The validation of Satellite Ground Control Station models was carried out in order to ensure that the model assumptions are correct, complete and consistent. The models were validated using computer assisted investigation so as to enhance confidence in the models.

1.6.4 Applications of Satellite Ground Control Station Model

Some of the applications of models of satellite ground control stations are as follows:

(a) The linearized model of satellite ground control station (GCS) can be used for the control of Unmanned Aircraft System (i.e. an unpiloted aircraft), formerly known as

unmanned aerial vehicle (UAV). UAVs can be remote-controlled and fly autonomously based on pre-programmed flight plans. UAVs are currently being used in a number of military roles, including reconnaissance and attack and for civil applications such as firefighting when a human observer would be at risk, police observation of civil disturbances and crime scenes, and reconnaissance support in natural disasters.

(b) It can be used to study real-time control of the satellite.

(c) It can also be used to study control of missile and rocket launch.

(d) It can be used to study operations of space robotics.

1.7 Project Scope

In this project, linearized mathematical model of Satellite Ground Control Station was developed. The system would allow for basic control of the ground station hardware such as radio and antenna. Furthermore, the system would enable an operator to have a wider exposure about how to model, linearize and validate a Satellite Ground Control Station. Emphasis was put on flexibility and robustness of the system.

There are five chapters to describe the modelling, linearization and validation of satellite ground control station system in this thesis.

- Chapter One introduces the basic knowledge of satellite communications system, with particular emphasis on satellite ground control station.
- Chapter Two highlights the important features of the satellite that have to be tracked and controlled by the Satellite Ground Control Station. It, thereafter,

reviews some of the previous works related to the modelling of Satellite Ground Control Station.

- Chapter Three concentrates on the modelling and linearization of Satellite Ground Control Station. It also gives detailed design of each part of the system.
- Chapter Four describes the validation of the models of Satellite Ground Control Station developed.
- Chapter Five discusses the conclusion and recommendations.

CHAPTER TWO

2.0 REVIEW OF RELEVANT LITERATURE

2.1 Attitude and Orbit Control System (AOCS)

The attitude and orbit control system (AOCS) of a satellite system provides attitude information and maintains the required spacecraft attitude during all phases of the mission, starting at spacecraft separation from the launch vehicle and throughout its operational lifetime. The system consists of redundant microprocessor-based control electronics, sun and earth sensors, gyros, momentum wheels (MWs), a reaction wheel (RW), magnetic torquers, thrusters, and solar array and trim tab positioners (Timothy *et al.*, 2003). Much of the control hardware is redundant in order to guarantee a reliable control system despite potential hardware failure (Marcel, 1997).

The attitude and orbit of a satellite must be controlled so that the satellite's antenna points toward the earth and for the user to know that the user knows where in the sky to look for the satellite. This is particularly important for GEO satellites since the earth station antennas that are used with GEO satellites are normally fixed and movements of the satellite away from its appointed position in the sky will cause a loss of signal.

2.1.1 Attitude Control System

Attitude of a spacecraft refers to its orientation in space. Attitude control is necessary so as to ensure that directional antennas point in the proper directions. To exercise attitude

script/program based autonomous control. Each of these modes supports the ability to configure and monitor station equipment as well as to conduct command and telemetry operations with spacecraft. Mercury accomplishes this by providing a centralized software interface to control all ground station equipment, software routines to automate station operation, and an internet gateway to access the centralized interface.

Figure 2.3 shows the Mercury Control System. It was developed to support advanced command and telemetry operations. The Mercury system is being implemented on Stanford's Space System Development Laboratory (SSDL)'s OSCAR-class amateur radio ground station. Mercury was used to test two SSDL microsatellites prepared for launch in 1999.

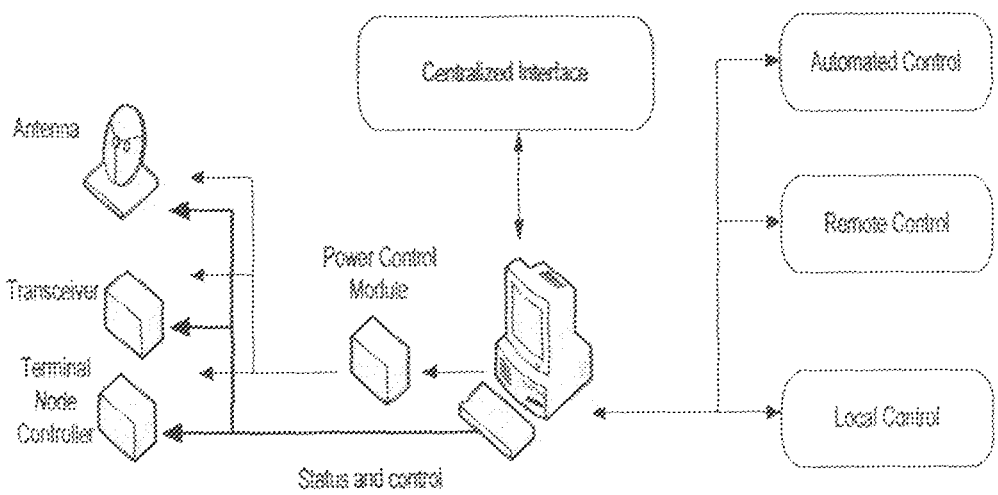

Fig. 2.3: Mercury Control System [James and Christopher, 2002]

The paper further described the design and operation of the Mercury system, its implementation in the SSDL OSCAR station, its use to conduct mission operations with

SSDL micro satellites, its role in SSDL's multi-satellite and multi-ground station mission operations architecture.

2.6 Design and Prototyping of High Availability Architecture for Satellite Ground Control System

A Satellite Ground Control System (SGCS), that monitors and controls a geostationary satellite 24 hours a day, was designed by In et al (2005) using distributed architecture so as to ensure high level of availability. The SGCS for communication, ocean, and meteorological satellite (COMS) is currently being developed in Korea and being implemented to satisfy high availability, expansibility, and compatibility in design. In order to implement the system architecture to meet these characteristics, In et al introduced the concept of the real-time distributed system structure based on fault detection and recovery, data replication and sharing using CORBA middleware and redundancy scheme. The paper also described down-size hardware and software configuration to perform the mission operation of geostationary satellite, and the prototyped services for 24-hour operation.

2.7 Ground Station Design for UWE-1

A new software called GSS2 (Ground Station Software 2) and its internal mechanism was presented by Yingie (2006). GSS2 was designed for ground station systems that carry out multiple ground station functions for UWE-1 (University of Würzburg's Experimental) satellite, such as orbit calculation, satellite tracking, telemetry processing

and display, alarm and event processing etc. UWE-1 is a CubeSat built by students of the University of Würzburg for testing adaptations of internet protocols to the space environment and was launched in Russia.

A Distributed System with Hyper-Threading (HT) Model was introduced by Yingie (2006) to optimize the performance and make the whole system easier to maintain and improve. His goal was to develop flexible stations with multi-mission capabilities. The GSS2 is an intelligent ground station system designed to provide a reliable, high quality, satellite data collection and distribution service. In the paper, the following steps were used to describe the GSS2: Mathematical Model, Map Projections, System Model, Numerical Methods and Implementation details.

2.8 Control System for Unmanned Aerial Vehicles (UAV)

An open project dealing with autopilot design for autonomous Unmanned Aerial Vehicles was introduced by Ondrej *et al.* (2005). In their paper, they proposed networked hierarchical distributed control system, and its hardware and software structure were briefly described. Mathematical model of a small rotorcraft was presented and identification methodology and state estimation using Extended Kalman Filter were discussed. Control algorithms, based on PI, LQG and SDRE approaches, focused on rotorcraft UAVs were proposed, including a complex hierarchical autopilot design. Real data, measured during test-flights of an experimental UAV, are also presented.

2.9 Cost Reduction Design Study for Spacecraft Control System

The aim of this design is to reduce the cost of spacecraft control system. National Space Development Agency of Japan (NASDA) selected two targets for cost reduction: construction and operating costs. Being one of the three elements composing NASDA's Tracking Control System, Spacecraft Control System is a system that controls the operation control work of spacecraft. Conventional spacecraft control systems were divided into several sub-systems (real-time processing, analytic processing, planning processing, etc.), which were combined for use in spacecraft control systems and were installed on the hardware (mini-computer, mainframe computer, work station, etc) when they were required. Since NASDA's spacecraft in recent years are no longer produced as a series as before and since the target for spacecraft control systems is expanding the experimental mission (moon exploration, etc.), the complexity and variety of spacecraft control is increasing (Miyuki *et al.*, 2000).

Cost reduction is the aim of spacecraft control systems and the targets for cost reduction in the next generation spacecraft control system are the construction costs and operation costs. The operation cost is accounted for mainly by the cost associated with personnel expenses and the running cost. However, the paper focused on the methods of reducing the number of operators. In order to operate with fewer numbers of personnel, it is essential to establish automation. A method for automation and reducing operator's load by ground system was presented in the paper (Miyuki *et al.*, 2000).

control, there must be available some measure of a satellite's orientation in space and of any tendency for this to shift. Usually, the attitude control process takes place aboard the satellite, but it is also possible for control signals to be transmitted from earth, based on attitude data obtained from the satellite (Dennis, 2002). There are two ways to make a satellite stable in orbit. The first way is to rotate the body of the satellite in order to create a gyroscopic force that provides stability of the spin axis and keeps it pointing in the same direction as in the case of spinner satellites. The second way is to stabilize the satellite by one or more momentum wheels as in the case of a three-axis stabilized satellite (Timothy *et al.*, 2003).

Spacecraft attitude is usually given in terms of a set of reference Cartesian axes (X_R, Y_R, Z_R) as shown in Figure 2.1. The forces on the satellite are also indicated in the figure. The Z_R axis is directed towards the center of the earth and is in the plane of the satellite orbit. It is aligned along the local vertical at the satellite's sub-satellite point. The X_R axis is tangent to the orbital plane and lies in the orbital plane. The Y_R axis is perpendicular to the orbital plane. Rotation about the X_R axis is defined as *roll*, about the Y_R axis is defined as *pitch* and about the Z_R axis is defined as *yaw*. The Z axis is usually directed toward a reference point on the earth, called the *Z-axis intercept*. The location of the Z-axis intercept defines the pointing of the satellite antennas; the Z-axis intercept point may be moved to repoint all the antenna beams by changing the attitude of the satellite with the attitude control system (Dennis, 2002; Timothy *et al.*, 2003; James and Wiley, 1999).

2.10 A Ground Control System for CBERS 3 and 4 Satellites

The ground control of the third and fourth China-Brazil Earth Resources Satellites (CBERS 3 and 4) was carried out by a new system under development at INPE (Paulo *et al.*, 2003). This system includes new technologies to reduce costs and development time of future ground system projects, through shared or adaptable software. Taking advantage of the experience gained in earlier ground control systems, the entities related to satellite operations activities have been modeled as metadata. This modeling approach is expected to increase the systems's reusability and reduce the efforts required to make changes.

Whenever modeling costs of entities via metadata are unfeasible, their programming interfaces are defined by Design Patterns in order to facilitate future changes. Furthermore, the telecommand and telemetry subsystems architecture includes a processing kernel, which can be shared with Electrical Ground Support Equipment (EGSE) and satellite simulation software. In the future, this system will be upgraded to include Artificial Intelligence (AI) techniques, like planning and preparing flight operation plans for the routine phase of the missions. The engineers in charge of planning the satellite operations will use tools developed with Dynamic Object Model technology to define the operations activities. Through the high-level script language supplied by these tools, the engineers will be able to define and/or change the knowledge database of operations activities, without requiring specific software development for each satellite.

The paper further presents the modeling of the operations entities to increase the satellite control system`s reusability and provide software that may be used by the control center,

testing (EGSE), and simulation systems. The paper also shows how the Dynamic Object Model and AI technologies will be added to the system in order to automate the control center operations, thereby reducing operations cost. The automation solution adopted allows transferring control to the manual mode whenever necessary.

2.11 Analysis of Satellite Ground Station Control System Using Java and Mercury Software

Two existing ground station softwares analyzed by Yu (2005) are: Mercury system and Java Satellite Ground Station (JStation). The Mercury system provides command console control, script program based autonomous control, and remote access client for commanding a controlling satellite ground stations via the Internet. The goals/aims of developing the Mercury system are to reduce the cost of operating space missions and to increase mission yields and capabilities. The Java Satellite Ground Station is a software package designed to operate the digital store-and-forward satellite which is written in java and is portable across multiple software and hardware platforms.

Through the unit testing, integration testing and on-site testing, all the functionalities of the ground station control system were tested. Figure 2.4 shows the context diagram of the control system. The automation of the ground station control system executed in the project provided a simple and flexible solution to be used for small student satellites.

The major services of the ground station like satellite tracking, data and protocol handling and logging were accomplished in the implementation phase of the project. The system

also implemented a prototype of the protocols which were used to set up the communication link with the satellite. A flexible alternative manual operation was also accomplished to allow for manual control of the system. The remote access and automation of the control system frees the operators from physically being at the ground station and give them more flexible work space.

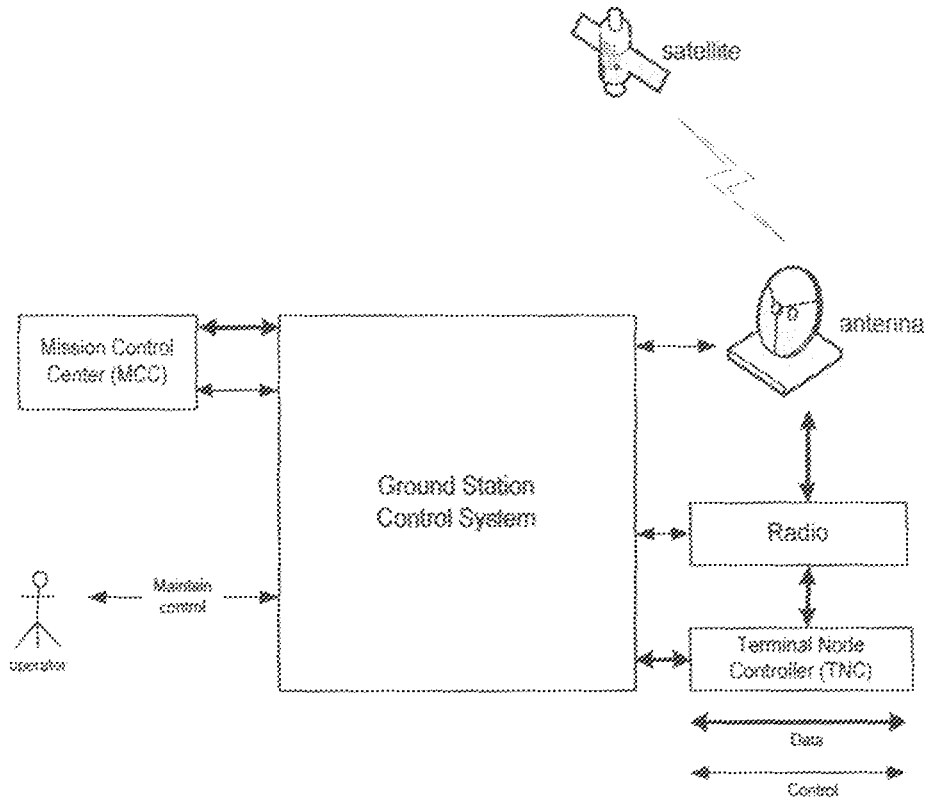

Fig. 2.4: Context diagram of control system [Yu, 2005]

As a simple and flexible architecture for a small-scale ground station system, four major components were proposed: a ground station control system, the real-time communication path with the satellite, a satellite mission control center for uplink and downlink communication with the satellite and pre- and post-processing components. A generic ground station developed was explained by Yu (2005). The system was designed

to allow for basic control of the ground station hardware such as radio and antenna. Furthermore, the system designed ensures that an external satellite mission control center can set up sessions automatically for controlling of satellite.

2.12 AM18 Ground Control Station for Unmanned Aerial Vehicles

The objective of the project was to develop a Ground Control Station (GCS) for multiple Unmanned Aerial Vehicles (UAVs) as stated by Ong (2005). The GCS was designed to coordinate the takeoff, search, landing and recovery of the UAVs. The GCS was based on a laptop with commercial-off-the-shelf (COTS) wireless modem for communication and video link. A TCP/IP sockets code for wireless communications between two PCs was implemenented. The program was built with open source TCP/IP socket code. The graphical user interface (GUI) designed for the project was coded with FLTK – a C++ GUI toolkit. The GUI displayed the packets sent by an onboard program, UAVclient, which interfaces with the UAV autopilot. Also, the GUI reproduces this information on a map image of the area of operations. The entire GUI was built from ground up.

The project was grouped into three divisions: Automatic Targeting System (ATS), Collision Avoidance System and Ground Control System. It was also divided into three different milestones: Communications Protocol (basic two-way communications between flight control system on robotic aerial platform and ground control system), Graphical User Interface (including Map display and mission profile graph) and field testing. Field testing conducted proved that the wireless communications do not suffer. The Graphic User Interface built was robust and can be readily customised by subsequent developers

for their specific use. The *UAVclient* program also provided a structure for future development to continue after the MP2028g or MP2128g SDK has been obtained.

2.13 An SDR – Based Architecture Ground Station for Small Satellite Tracking

In his paper, Chiu-Teng (2004) presented a software defined radio (SDR)-based architecture to realize ground station functions so as to enhance the tracking capability and overall workload. A multi-band receiving capability is implemented by the down-converter block, using band-pass sampling theorem, in the SDR. Signals in distinct frequencies can be extracted simultaneously by short-time Fourier transform and digital filter blocks. The contact duration and probability were shown to be extendable by designing an appropriate hand-over function through a ground station network. With the proposed architecture, ground stations can track several satellites simultaneously and record the signals for post processing. Furthermore, tracking errors caused by Doppler shift, clock drift, and interferences can be mitigated. In the paper, a realization of the SDR-based ground station was provided. The effectiveness in improving the overall tracking capability was also demonstrated.

The SDR-based approach is flexible so that the tracking performance can be made adaptively to account for the demanding tasks in satellite tracking, especially during the early-orbit phase. All these changes were achieved without hardware modification. By the proposed approach, a part of the problem of satellite tracking in early orbit phase was solved. In addition, the approach can also be used to prevent interference in ordinary

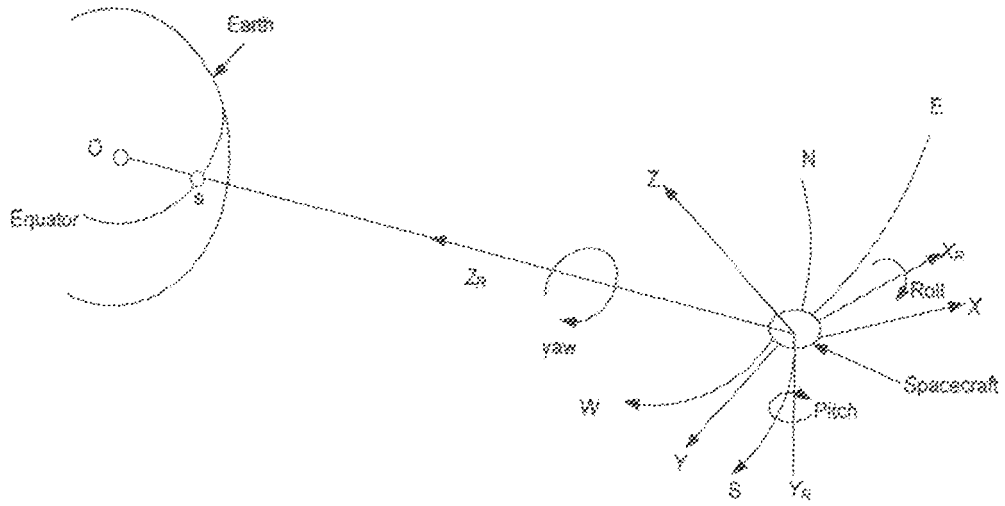

Fig 2.1: Cartesian axes and Forces on a Satellite (Timothy *et al.*, 2003)

2.1.2 Orbit Control System

Spacecraft orbit control requires accurate determination of the spacecraft's state, consisting of the position and velocity of the spacecraft at a specified time. Orbit control is carried out whenever there is need to overcome secular orbit perturbations or to maintain relative orientation of satellites to the Earth. A geostationary satellite can be subjected to several forces that tend to accelerate it away from its required orbit. The most important, for the geostationary satellite, are the gravitational forces of the moon and the sun, which cause inclination of the orbital plane to change, the non-spherical shape of the earth around the equator which causes drift of the sub-satellite point, and solar radiation pressure which causes change in eccentricity (Marcel, 1997).

Figure 2.2 shows an inclined orbital plane. For the orbit to be truly geostationary, it must lie in the equatorial plane, be circular, and have the correct altitude. The various forces acting on the satellite will steadily pull it out of the correct orbit; it is the function of the

orbit control system to return it to the correct orbit. The orbital control system of the satellite must be able to move the satellite back into the equatorial plane before the orbital inclination becomes excessive (Timothy *et al.*, 2003).

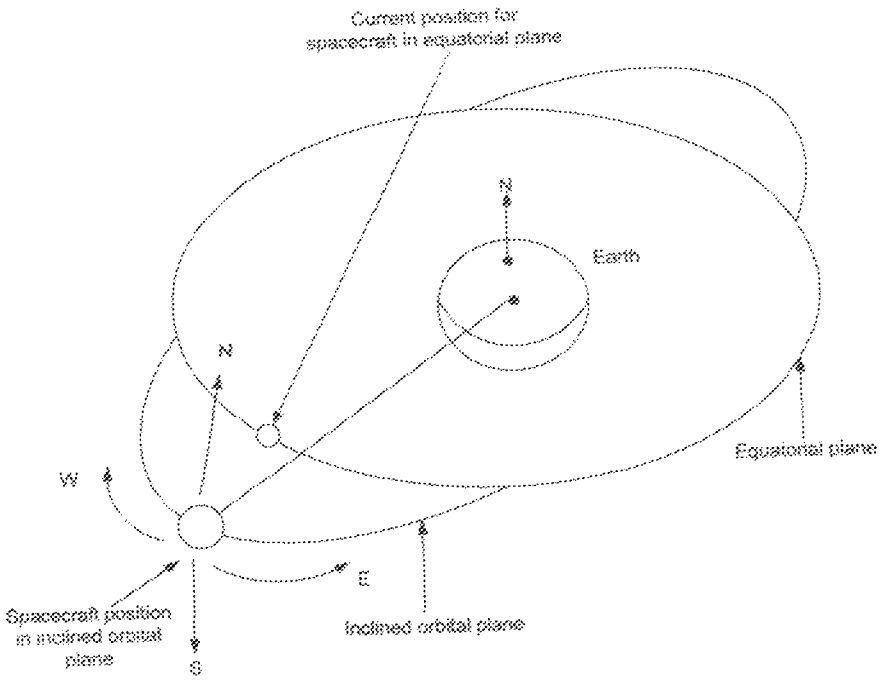

Fig 2.2: Satellite in an inclined orbit

2.2 Development of an Unmanned Aerial Vehicle (UAV) Ground Control Station

The design and development of Ground Control Station (GCS) for the control and analysis of unmanned aerial vehicle was explained by Philip (2002). Initially, the primary control for the UAV has been the integration of a commercial joystick. The main data that has been displayed on the flight data screen comes from a sensor on the aircraft

known as an attitude and heading reference sensor or AHRS. The whole system was placed in an aluminium rack and secured to the floor of a Caravelle car. The software used, LabVIEW, enabled the development of the Unmanned Aerial Vehicle to be quick and simple. It displayed accurately the output of both the flight data and graphs.

2.3 Simulation System of Telemetering and Telecontrol for Unmanned Aerial Vehicle (UAV)

The "Simulation System of Telemetering and Telecontrol for Unmanned Aerial Vehicle (UAV)", written by Ding et al (2006), is composed of tracking, navigation, telecontrol, telemetering, and flight control. The Unmanned Aerial Vehicle (UAV) referred to in the paper "Simulation System of Telemetering and Telecontrol for Unmanned Aerial Vehicle (UAV)" is capable to observe the earth and has wide applications and large quantities. They can be used in many ways such as reconnaissance and surveillance, attack on the ground, fire-proof forest, and marine search and rescue, and so on. This kind of UAV usually consists of telecontrol, telemetering, tracking, navigation, and image transmission system. Telecontrol system sends instructions to UAV by the telecontrol transmitter on the ground station, whose main function is to control UAV flight and mission device (such as camera, infrared scanner, and operating platform). Telemetering system transmits the information including flight attitude of UAV, flight parameters, and device state to the ground station by telemetering transmitter, which is collected by sensors in UAV (Ding *et al.*, 2006).

The telemetering and telecontrol system for UAV is very complex. Therefore, in order to aid the development of new types of UAV that are better and swifter, telemetering and control system of simulation was provided by (Ding *et al.*, 2006). The system consists of the control cabinet of flight, the control cabinet of navigation, and the control cabinet of mission. The simulation system is consists of

a) simulation of telecontrol and flight control system for the simulation of telecontrol instruction;
b) simulation of telemetering system for the simulation of attitude parameter, speed and altitude of UAV, engine parameter and GPS parameter;
c) simulation of tracking and positioning for UAV for the simulation of tracking and positioning parameter of UAV; and
d) simulation of target observation and tracking for the simulation of target parameter.

They, therefore, show that through the simulation of telemetering and telecontrol for unmanned aerial vehicle a better type of UAV can be obtained and the quality of telecontrol and telemetering will be greatly improved. The simulation system of telemetering and telecontrol for UAV can be used not only in development of UAV, but also in training simulation.

2.4 Low Cost Satellite Ground Control Facility Design

Scott and John (1993) focussed the design approach of "Low Cost Satellite Ground Control Facility Design" on the common areas of satellite operations command and control, tracking, subsystem analysis (including telemetry processing), system planning

and scheduling and orbit determination and maintenance. Specific satellite mission applications and operations were isolated from the remainder of the design to allow application to a broad variety of satellite systems. A low cost "generic" approach, which allows for phased implementation of system changes with minimal impact to on-orbit assets and mission performance, was developed. The goals of this approach are to provide the capability for growth, maintainability and operability of the satellite system. A brief discussion of satellite systems, followed by the introduction of the general functions of any satellite control facility, set the stage for the overall design approach used. The factors that define the design along with the key design features were presented in the paper with a final discussion of each product available in each functional area.

The paper showed the viability of designing a low cost (in a relative sense) satellite ground control facility, taking advantage of recent technological achievements and availability of Commercial Off The Shelf (COTS) support products. A number of commercially available Satellite Control "packages" were compared to the fundamental functional requirements and low cost design approach objectives. The application of these "packages" to real operational systems is relatively limited, but as need and commercial potential increase so will the use of these products.

2.5 Mercury Satellite Ground Station Control System

The design and operation of a "Mercury Satellite Ground Station Control System" was explained in the paper by James and Christopher (2002). Known as Mercury, this control system provides direct human console control, remote human tele-operation, and

ground station operation. The Doppler shift can be exactly known, not estimated by an orbit prediction software. It is very useful for the transmitter frequency tuning to uplink data. The signal`s baud rate is not limited by the TNC modem.

2.14 Low Cost Ground Station Design for Nano-satellite Missions

Tarun (2006), in his paper, explained the design and implementation of a fully capable ground station used to facilitate communications for nanosatellite missions. Nanosatellite missions by their very nature follow a philosophy of a low cost and rapid development cycle; and, as such, the ground station design is constrained to fall within this same framework. To demonstrate the feasibility of such an approach, an S-Band/UHF/VHF ground station design that was implemented for the CanX-2 nanosatellite mission at the University of Toronto Institute for Aerospace Studies Space Flight Laboratory (UTIAS/SFL) was discussed. The design utilizes a central TNC based on a GFSK modem and a single-board ARM computer running an open-source Linux kernel with all other software developed in-house. The TNC is responsible for (de)modulation, control of ground station hardware and the necessary orbital tracking of the spacecraft.

A commercially available actuator, used for antenna pointing, interfaces with a custom rotator controller that provides added mechanical fault detection. A GUI software application running on standard PCs acts as the satellite`s operating environment. This GUI connects to the ground station TNC using TCP/IP and even permits scientists to remotely control their own experiments onboard the satellite. The software and hardware used for this ground station was designed to be modular so that the system could be easily

modified and upgraded to meet the needs of future missions. The current ground station was successfully tested by tracking and receiving signals from other orbiting satellites. The successful implementation of the CanX-2 ground station demonstrated that for less than a few tens of thousands of Canadian dollars a highly capable ground station can be built to support a wide range of nanosatellite missions. The ground station model presented in the paper could be directly applied to almost any small satellite program wishing to implement their own ground station with minimal cost and complexity.

2.15 Transportable Orbital Tracking, Telemetry and Command System

The implementation of an automated ground-based telemetry, command, and Doppler system by NASA/Goddard Space Flight Center was explained by Powell (1993). Its function is to support the low-earth-orbiting satellite and sounding rocket programs. This fully transportable system can be configured with the capability to provide unmanned satellite support for seven days or operator-augmented automated sounding rocket launch and tracking support. An extensive overview of the evolutionary status and functional capabilities of such systems is provided.

2.16 A Self-Tuning Real-Time Orbit Determination System

Spacecraft orbit control requires accurate determination of the spacecraft`s state, consisting of the position and velocity of the spacecraft at a specified time. Automation of the control problem necessitates that this orbit determination be performed in real time, using a robust, self-correcting algorithm. Existing methods fail to meet these requirements in one or more respects. Most existing systems accumulate orbit data over an extended time span and then fit these data to an estimate of the orbital state. An

alternative approach uses a Kalman filter to estimate the spacecraft's state as data is collected. The former approach fails to meet the near real-time requirements of an autonomous system. The latter becomes stiff as time progresses, and tends to lose the ability to adjust to small changes in the spacecraft's environment. Darrel *et al.* (2001) experimented with a neural network placed in control of a Kalman filter orbit determination system in order to evaluate the feasibility of such an autonomous tool.

The location and motion of a spacecraft must be estimated accurately in order to control the spacecraft during execution of its mission. The advent of satellite formations and constellations makes this task even more formidable. Not only must each satellite be controlled to a precise orbit, but the location and movement of the satellites relative to one another must also be controlled to meet mission requirements. AI Solutions in cooperation with the National Aeronautics and Space Administration's (NASA) Goddard Space Flight Center (GSFC) is developing systems that would address the core automation needs of the aerospace community in these regimes. As part of these development efforts, AI Solutions is developing a real time orbit determination system under a small business innovation research (SBIR) contract. This system uses a Kalman filter to estimate orbital states as measurement data are collected. The Kalman filter is monitored and controlled by an artificial neural network (Darrel *et al.*, 2001).

The orbit determination problem, that is, the problem of finding the parameters that determine the satellite's position and velocity in space at a specified time is a well understood problem in spacecraft flight dynamics. Tools that estimate orbital states using

current technologies include GSFC's Goddard Trajectory Determination System (GTDS) and Analytical Graphics' Precision Orbit Determination System (PODS). These systems estimate orbits using input measurement data, and arrive at acceptably close approximations to the orbital state to perform orbit planning and science gathering activities. An integral piece of the estimation of accurate orbit states using these tools is tuning the system to handle anomalous and spurious data. These data are traditionally handled by an analyst inspecting the data, categorizing it, and setting the orbit determination parameters appropriately. After the data have been processed, an analyst examines the fit of the estimated orbit to the measured data, the analyst uses the difference between the estimated orbital state and the measured orbital state, referred to as the measurement residuals, to judge the quality of the estimated orbit (Darrel *et al.*, 2001).

2.17 Electromagnetic Noise of Satellite Ground Station

Liu and Wang (1997) having comprehensively studied the link formulas and some engineering experiences on satellite receiving, and through strict mathematical deductions, set up a new mathematic model on the antenna diameter and unweighted video given as

$$\frac{S}{N}: D = 10^{x} \tag{2.1}$$

where, $x = 0.05S/N - 0.05EIRP - 10.91598564 - 0.5L_g\eta + L_g d + 0.05\Delta L + 0.5L_g(T_a + T_r) - L_g\Delta f_v + 1.5L_g f_v - 0.05F$

D = caliber size (diameter) of the satellite receiving antenna (m).

S/N = video signal to noise ratio (dB).

$EIRP$ = Equivalent Isotropic Radiated Power (dBw).

L_g = Losses

η = antenna efficiency, usually is taken as 0.65 in engineering.

d = distance from satellite to ground station (m).

ΔL =down-going additional loss (dB).

Δf_v = video frequency deviation (Hz).

f_v = Max. video frequency (Hz).

F = deaccentuation improving factor.

T_a = antenna noise temperature.

T_r = HF tuner noise temperature

The un-weighted video S/N can directly indicate the quality of pictures (which is usually required by users). The establishment of this formula gives a direct relationship between the antenna diameter D and the S/N, and makes it possible to draw a $D - S/N$ curve, showing that the $D - S/N$ relationship is not a linear one. The satellite receiving antenna costs one-third of the total ground station, and the cost of the antenna is proportional to the square of the antenna diameter D. Therefore, the accuracy of antenna diameter is rather critical. The designer may accurately and quickly find out the D value by using the $D - S/N$ curve when designing a specific satellite ground receiving station [Liu and Wang, 1997].

CHAPTER THREE

3.0 MATERIALS AND METHODS

Satellite Ground Control Station is composed of various components which interact with one another in different ways, but within the limits imposed by certain strategies used to control the system as a whole. Mathematical models of various components that make up satellite ground control station are presented. The models are validated in order to ensure that the model assumptions are correct, complete and consistent and to enhance confidence in the model. The schematic diagram of Satellite Ground Control Station developed is shown in Figure 3.1

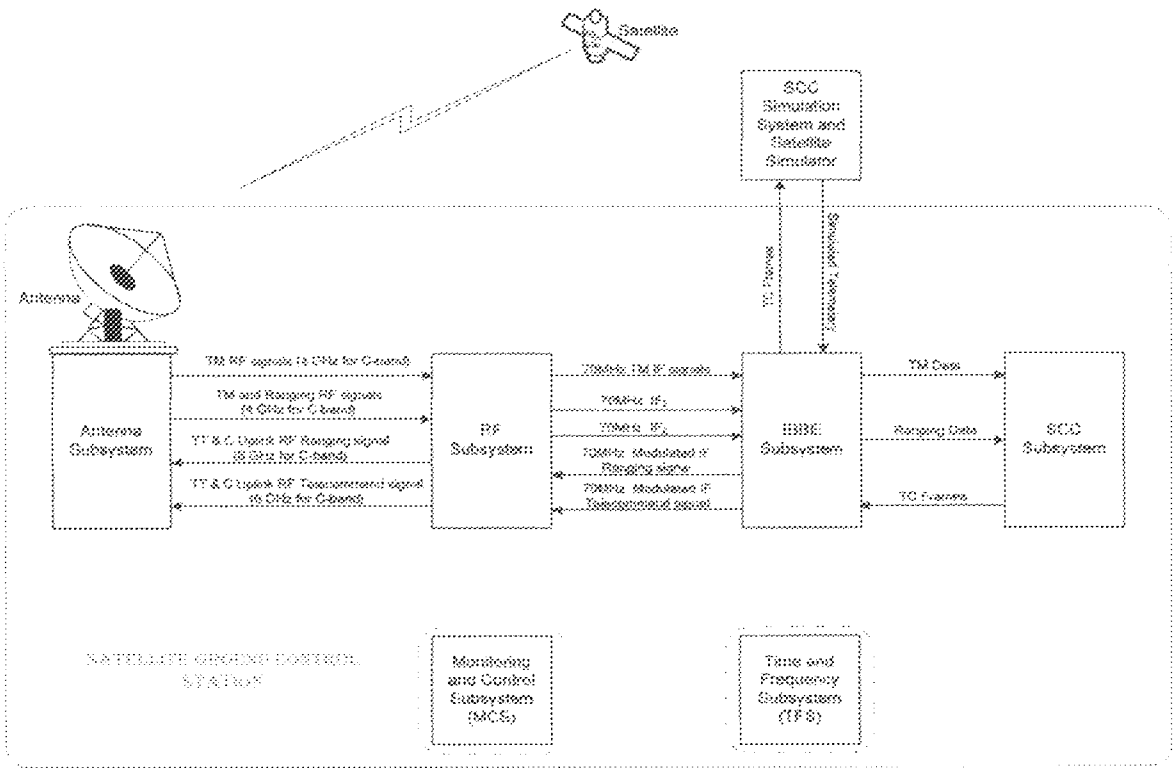

Fig. 3.1 Schematic Diagram of Satellite Ground Control Station

Satellite Ground Control Station is a complex system. To understand and control it, therefore, one must obtain its quantitative model. Because the system under consideration is dynamic in

nature, the descriptive equations are usually differential equations. The complexity of the system necessitates the introduction of assumptions concerning the system operation. Therefore, it is very useful to consider the physical system, delineate some necessary assumptions, and linearize the system. Then by using the physical laws describing the linear equivalent system, we can obtain a set of linear differential equations.

A great majority of physical systems are linear within some range of the variables. However, all systems (e.g. Satellite Ground Control Station) ultimately become non-linear as the variables are increased without limit (e.g. introduction of noise and interference). Therefore, the question of linearity and the range of applicability must be considered for the system. A linear system satisfies the properties of superposition and homogeneity.

The linearity of a satellite ground control station is assumed over a reasonably large range of variables. The non-linear system, Satellite Ground Control Station, is linearized assuming small signal conditions and using ordinary differential equations which can be easily modelled and solved using standard methods (Bender, 1978).

Bender stated that, the cosine function $y = cosy_1$ is the solution of the differential equation

$$\frac{d^2y}{dy_1^2} = -y = -cosy_1 \qquad (3.1)$$

This differential equation is equivalent to the linear system

$$z = \frac{dy}{d\gamma_1} = -sin\gamma_1 \; and \; \frac{dz}{d\gamma_1} = \frac{d^2y}{d{\gamma_1}^2} = -y = -cos\gamma_1 \qquad (3.2)$$

Therefore, $cos\gamma_1$ can be substituted with $-dz/d\gamma_1$ and this approach was used throughout the modelling of Satellite Ground Control Station. The central angle γ_1 is the angle at whcih a Satellite Ground Control Station must be located in order to be able to see and track satellite. In this thesis, the central angle γ_1 under the consideration lie within the inequality $0 \leq \gamma_1 \leq 81.3^0 \; i.e. \; (0 \leq \gamma_1 \leq 1.4191 \; rad)$.

3.1 Antenna Subsystem

Each of the components of the antenna subsystem is modelled and linearized as presented in the sub-sections below.

3.1.1 Antenna Look Angles

To ensure that an earth station antenna is aligned with the satellite it wants to track and be able to communicate with it i.e. have line of sight with the satellite, two angles must be determined: the azimuth angle and the elevation angle. These are the co-ordinates to which an earth station antenna must be pointed in order to communicate with a satellite. Azimuth is measured eastward (clockwise) from geographic north to the projection of the satellite path on a (locally) horizontal plane at the earth station. Elevation is measured upward from the local horizontal plane at the earth station to the satellite path.

Figure 3.2 shows the geometry of the range and elevation angle calculation. In this geometry, two models of satellite ground control stations are presented. Also, one satellite ground control station will be used as the main station while the other will be used as the back-up or redundnat system. The redundant system will take over the control of the satellite whenever the main control system fails or its link is obstructed by the rain attenuation. The models will aid availability of the system at all time. The two ground control stations are linked by a geostationary satellite for continuous communications.

To track a satellite three parameters are needed: Range, Azimuth angle and Elevation angle. Each of them is modelled mathematicaly using the models for Satellite Ground Control Stations X and Y shown in Figure 3.2.

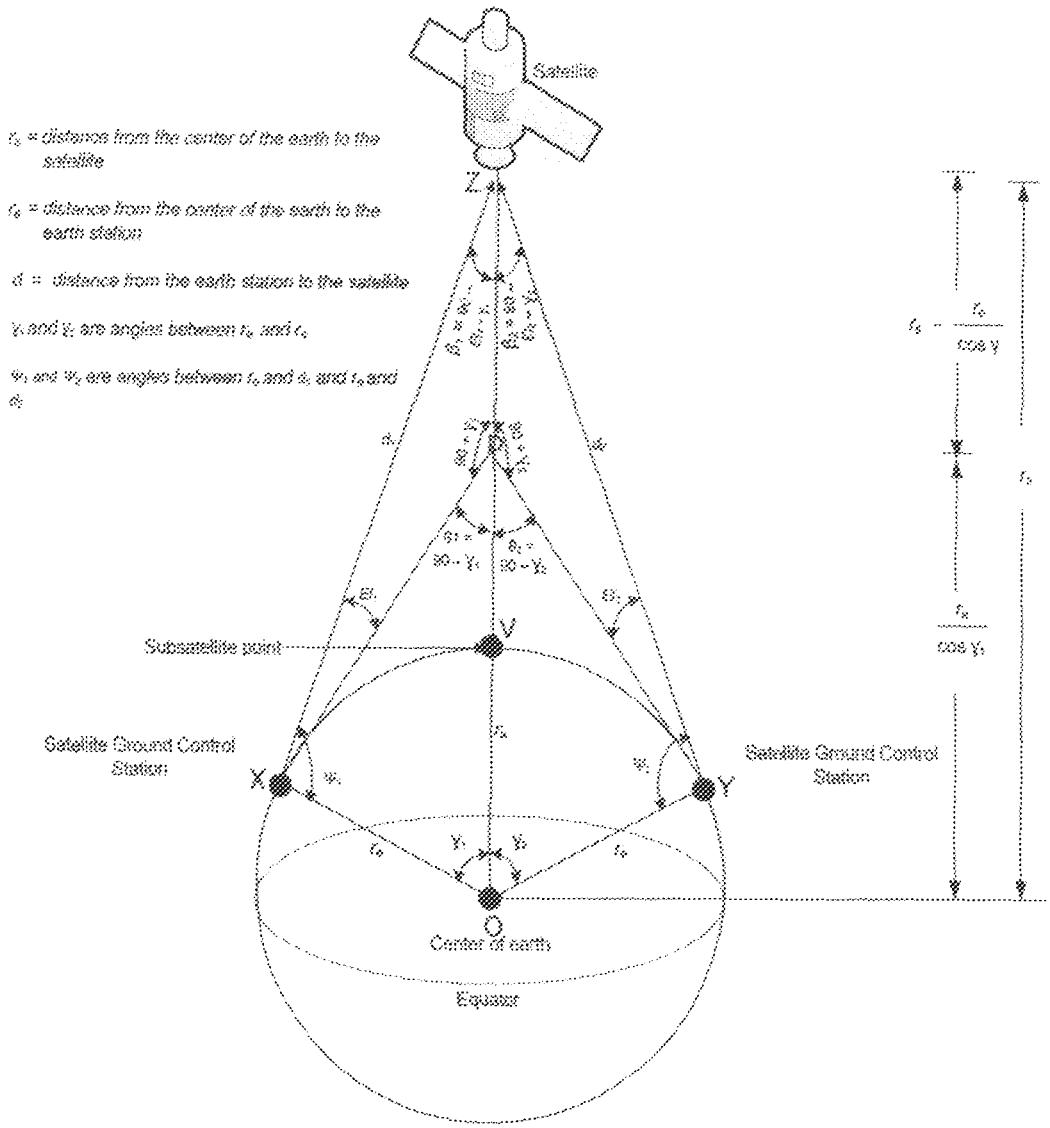

Fig 3.2: Geometry of the range and elevation angle calculation

Model 1: For Satellite Ground Control Station X

From ΔZXO of Fig. 3.2: Using cosine formula, we have

$$d_1^2 = r_s^2 + r_e^2 - 2r_e r_s cos\gamma_1 \tag{3.3}$$

$$d_1 = [r_s^2 + r_e^2 - 2r_e r_s cos\gamma_1]^{\frac{1}{2}} \tag{3.4}$$

$$d_1 = r_s\left[1 + \left(\frac{r_e}{r_s}\right)^2 - 2\left(\frac{r_e}{r_s}\right)cos\gamma_1\right]^{1/2} \tag{3.5}$$

Similarly, from ΔZXO of Fig. 3.2

$$r_e^2 = d_1^2 + r_s^2 - 2d_1 r_s cos(90 - \gamma_1 - El_1) \tag{3.6}$$

$$= d_1^2 + r_s^2 - 2d_1 r_s \sin(\gamma_1 + El_1) \tag{3.7}$$

$$r_e = [d_1^2 + r_s^2 - 2d_1 r_s \sin(\gamma_1 + El_1)]^{\frac{1}{2}} \tag{3.8}$$

$$= d_1\left[1 + \left(\frac{r_s}{d_1}\right)^2 - 2\left(\frac{r_s}{d_1}\right)\sin(\gamma_1 + El_1)\right]^{1/2} \tag{3.9}$$

Also, from ΔZXO of Fig. 3.2

$$r_s^2 = r_e^2 + d_1^2 - 2d_1 r_e \cos(90 + El_1) \tag{3.10}$$

$$r_s = [r_e^2 + d_1^2 + 2d_1 r_e \sin El_1]^{1/2} \tag{3.11}$$

$$r_s = r_e\left[1 + \left(\frac{d_1}{r_e}\right)^2 + 2\left(\frac{d_1}{r_e}\right)\sin El_1\right]^{1/2} \tag{3.12}$$

Applying sine formula to ΔZXD of Fig. 3.2 we have

$$\frac{\left(r_s - \frac{r_e}{cos\gamma_1}\right)}{sinEl_1} = \frac{d_1}{\sin(90 + \gamma_1)} \tag{3.13}$$

$$sinEl_1 = \frac{\left(r_s - \frac{r_e}{cos\gamma_1}\right)\sin(90 + \gamma_1)}{d_1} \tag{3.14}$$

Therefore,

$$El_1 = \sin^{-1}\left[\frac{\left(r_s - \frac{r_e}{cos(\gamma_1)}\right)\sin(90+\gamma_1)}{d_1}\right] = \sin^{-1}\left[\frac{(r_s cos(\gamma_1) - r_e)}{d_1}\right] \quad (3.15)$$

Assuming the satellite ground control station being modelled is a linear system and taking

$$y = cos\gamma_1 \text{ and } dz/d\gamma_1 = -cos\gamma_1 \quad (3.16)$$

then d_1 in *Eq.* (3.3) can be linearized as

$$d_1{}^2 = r_s{}^2 + r_e{}^2 + 2r_e r_s \frac{dz}{d\gamma_1} \quad (3.17)$$

Therefore, the differential equation describing the dynamic performance of Satellite Ground Control Station is expressed as

$$\frac{dz}{d\gamma_1} = \frac{1}{2r_e r_s}\left[d_1{}^2 - r_s{}^2 - r_e{}^2\right] \quad (3.18)$$

The rate of change of d_1 with respect to γ_1 is obtained by differentiating *Eq.* (3.5) with respect to γ_1

$$\frac{d(d_1)}{d\gamma_1} = r_e \cdot \frac{1}{2} \cdot \left[1 + \left(\frac{r_e}{r_s}\right)^2 - 2\left(\frac{r_e}{r_s}\right)cos(\gamma_1)\right]^{-\frac{1}{2}} \cdot \left(-2\left(\frac{r_e}{r_s}\right) \cdot (-sin(\gamma_1))\right) \quad (3.19)$$

$$\frac{d(d_1)}{d\gamma_1} = \frac{r_e \cdot sin(\gamma_1)}{\left[1 + \left(\frac{r_e}{r_s}\right)^2 - 2\left(\frac{r_e}{r_s}\right)cos\gamma_1\right]^{\frac{1}{2}}} \quad (3.20)$$

Also, assuming the satellite ground control station being modelled is a linear system and taking

$$y = cos\gamma_1 \text{ and } dz/d\gamma_1 = -cos\gamma_1 \tag{3.21}$$

then *Eq.* (3.15) can be written as

$$El_1 = \sin^{-1}\left[\frac{-\left(\left(r_e\frac{dz}{d\gamma_1}\right) + r_e\right)}{d_1}\right] \tag{3.22}$$

Therefore, rearranging the expression in *Eq* (3.22), the differential equation describing the dynamic performance of satellite ground control station can be expressed as

$$\frac{dz}{d\gamma_1} = -\frac{1}{r_s}[d_1 \sin(El_1) + r_e] \tag{3.23}$$

The rate of change of El_1 with respect to the central angle γ_1 is obtained by differentiating *Eq.* 3.15 as shown below.

$$\frac{d(El_1)}{d(gamma)} = \frac{-r_s.sin\gamma_1}{(d_1{}^2 - r_s{}^2.cos^2\gamma_1 - 2r_e r_s.cos\gamma_1 - r_e{}^2)^{1/2}} \tag{3.24}$$

Figure 3.3 shows the position of a hypothetical geosynchronous satellite vehicle (GSV), subsatellite point (SSP), and an earth station (ES) all relative to Earth's geocenter. The SSP has 30^0E longitude and 0^0 latitude. The earth station has a location of 30^0W and 20^0N latitude. L_s and l_s are the latitude and longitude of the subsatellite point, while *Le* and *le* are the latitude and longitude of the Earth station respectively.

From ΔABC in Figure 3.3, using Napier's rule for a spherical right angled triangle which states that " the sine of an angle is equal to the product of tangents of the two adjacent angles", then

$$sin(L_e) = \tan A tan|B| = \tan A \tan|l_s - l_e| \tag{3.25}$$

Therefore,

$$\tan A = \frac{\tan|l_s - l_e|}{\sin(L_e)}, \text{then } A = tan^{-1}\left|\frac{\tan|l_s - l_e|}{\sin(L_e)}\right| \tag{3.26}$$

Once angle A is determined, the azimuth angle A_z can be found. Four situations must be considered, the results for which can be summarized as follows:

1. $L_e < 0;\ B < 0: A_z = A$
2. $L_e < 0;\ B > 0: A_z = 360^0 - A$
3. $L_e > 0;\ B < 0: A_z = 180^0 + A$
4. $L_e > 0;\ B > 0: A_z = 180^0 - A$

The rate of change of A with respect to L_e is obtained by differentiating *Eq.* (3.26)

$$\frac{dA}{dL_e} = -\frac{\cos(L_e).\tan|l_s - l_e|}{\sin^2 L_e + \tan^2|l_s - l_e|} \tag{3.27}$$

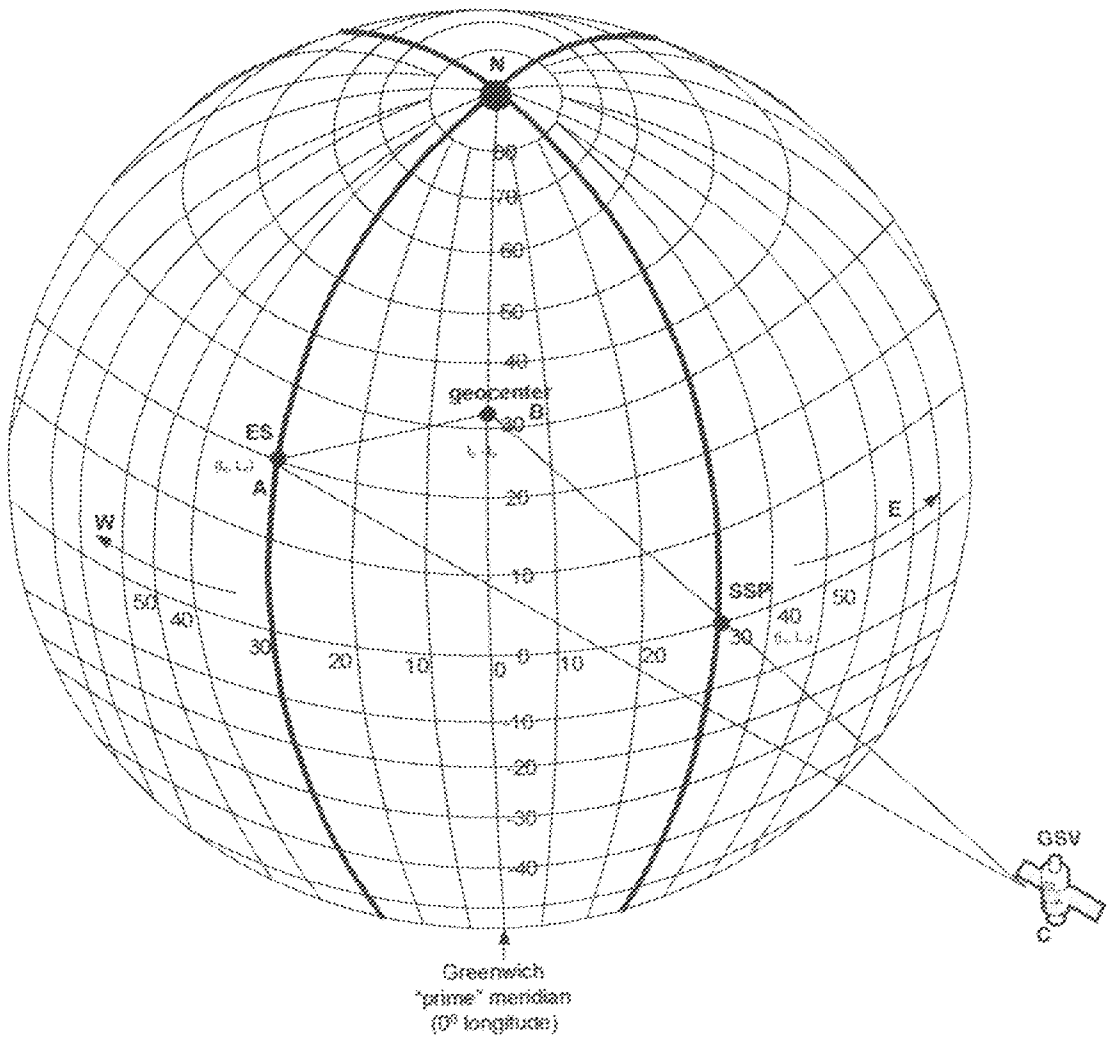

Fig. 3.3 Position of a hypothetical geosynchronous satellite vehicle (GSV), its respective subsatellite point (SSP), and an arbitrary selected earth station (ES) (Wayne, 2001)

Assuming the satellite ground control station being modelled is a linear system and taking

$$y = \sin(L_e),\ z = dy/dL_e = cos(L_e),\ \text{and}\ dz/dL_e = -\sin(L_e), \qquad (3.28)$$

then, *Eq.* (3.23) can be linearized as

$$-\frac{dz}{dL_e} = \tan A \tan|l_s - l_e| \tag{3.29}$$

Therefore, the differential equations describing the dynamic performance of satellite ground control station can be expressed as

$$\frac{dz}{dL_e} = -\tan A \tan|l_s - l_e| \tag{3.30}$$

Model 2: For Satellite Ground Control Station Y

From ΔZYO of Fig. 3.2: Using cosine formula, we have

$$d_2^{\,2} = r_s^{\,2} + r_e^{\,2} - 2r_e r_s cos\gamma_2 \tag{3.31}$$

$$d_2 = [r_s^{\,2} + r_e^{\,2} - 2r_e r_s cos\gamma_2]^{\frac{1}{2}} \tag{3.32}$$

$$= r_s\left[1 + \left(\frac{r_e}{r_s}\right)^2 - 2\left(\frac{r_e}{r_s}\right)cos\gamma_2\right]^{1/2} \tag{3.33}$$

Similarly, from ΔZYO of Fig. 3.2

$$r_e^{\,2} = d_2^{\,2} + r_s^{\,2} - 2d_2 r_s cos(90 - \gamma_2 - El_2) \tag{3.34}$$

$$= d_2^{\,2} + r_s^{\,2} - 2d_2 r_s \sin(\gamma_2 + El_2) \tag{3.35}$$

$$r_e = [d_2^{\,2} + r_s^{\,2} - 2d_2 r_s \sin(\gamma_2 + El_2)]^{\frac{1}{2}} \tag{3.36}$$

$$= d_2\left[1 + \left(\frac{r_s}{d_2}\right)^2 - 2\left(\frac{r_s}{d_2}\right)\sin(\gamma_2 + El_2)\right]^{1/2} \tag{3.37}$$

Also, from ΔZYO of Figure 3.2

$$r_s^{\,2} = r_e^{\,2} + d_2^{\,2} - 2d_2 r_e \cos(90 + El_2) \tag{3.38}$$

$$r_s = [r_e^2 + d_2^2 + 2d_2 r_e \sin El_2]^{1/2} \tag{3.39}$$

$$r_s = r_e\left[1 + \left(\frac{d_2}{r_e}\right)^2 + 2\left(\frac{d_2}{r_e}\right)\sin El_2\right]^{1/2} \tag{3.40}$$

Applying sine formula to ΔZYD of Fig. 3.2 we have

$$\frac{\left(r_s - \frac{r_e}{cos\gamma_2}\right)}{sinEl_2} = \frac{d_2}{\sin(90 + \gamma_2)} \tag{3.41}$$

$$sinEl_2 = \frac{\left(r_s - \frac{r_e}{cos\gamma_2}\right)\sin(90 + \gamma_2)}{d_2} \tag{3.42}$$

Therefore,

$$El_2 = \sin^{-1}\left[\frac{\left(r_s - \frac{r_e}{cos\gamma_2}\right)\sin(90 + \gamma_2)}{d_2}\right] = \sin^{-1}\left[\frac{(r_s cos(\gamma_2) - r_e)}{d_2}\right] \tag{3.43}$$

The rate of change of El_2 with respect to the central angle γ_2 is obtained by differentiating Eq (3.43) as shown below.

$$\frac{d(El_2)}{d(gamma)} = \frac{-r_s.sin(\gamma_2)}{(d_2^2 - r_s^2.cos^2\gamma_2 - 2r_e r_s.cos(\gamma_2) - r_e^2)^{1/2}} \tag{3.44}$$

Assuming the satellite ground control station being modelled is a linear system and taking

$$y = cos\gamma_1 \text{ and } dz/d\gamma_1 = -cos\gamma_1, \tag{3.45}$$

then d_2 in $Eq.$(3.31) can be written as

$$d_2^2 = r_s^2 + r_e^2 + 2r_e r_s \frac{dz}{d\gamma_2} \tag{3.46}$$

Quadrature phase branch: It mixes the local quadrature carrier signal generated by the local NCO and the input carrier signal. It also filters the sum signal through low pass filter and gives quadrature phase band signal. The local quadrature signal generated by NCO is (Xu, 2005)

$$s_o(t) = A_0 \sin(\omega_o t + \theta_0) \tag{3.73}$$

The input carrier signal is,

$$s_1(t) = A\cos\left[\omega_1 t + k_{p1} m_1(t) + k_{p2} m_2(t) + \theta_1\right] \tag{3.74}$$

The mathematical modelling of the mixture of $s_o(t)$ and $s_1(t)$ by the quadrature-phase branch is

$$\begin{aligned} s_1(t) \cdot s_0(t) &= A\cos\left[\omega_1 t + k_{p1} m_1(t) + k_{p2} m_2(t) + \theta_1\right] x A_0 \sin(\omega_o t + \theta_0) \\ &= A_0 A_1 \sin(\omega_o t + \theta_0) \cos\left[\omega_1 t + k_{p1} m_1(t) + k_{p2} m_2(t) + \theta_1\right] \end{aligned} \tag{3.75}$$

Using trigonometric functions, we have

$$\begin{aligned} s_1(t) \cdot s_o(t) = \frac{A_0 A_1}{2} sin\left[(\omega_1 + \omega_o)t + k_{p1} m_1(t) + k_{p2} m_2(t) + \theta_1 + \theta_0\right] \\ + \frac{A_0 A_1}{2} sin\left[(\omega_1 - \omega_o)t + k_{p1} m_1(t) + k_{p2} m_2(t) + \theta_1 - \theta_0\right] \end{aligned} \tag{3.76}$$

Low pass filter I removes the sum item and the resulting quadrature phase signal is,

$$Q_1(t) = A_1 sin\left[\Delta\omega t + k_{p1} m_1(t) + k_{p2} m_2(t) + \Delta\theta\right] \tag{3.77}$$

where, $\Delta\omega = \omega_1 - \omega_o$ and $\Delta\theta = \theta_1 - \theta_0$.

Low pass filter 1 filters $I_1(t)$ and produces $I_2(t)$ as shown in Fig. 3.8. Also, the second low pass filter 2 filters $Q_1(t)$ and produces $Q_2(t)$ as shown in Fig. 3.8 also. Through filtering by low pass filter 2 we get the signal $I_2(t)$ and $Q_2(t)$ shown below:

$$I_2(t) = A_1 cos[\Delta\omega t + \Delta\theta] \; and \; Q_2(t) = A_1 sin[\Delta\omega t + \Delta\theta] \tag{3.78}$$

$I_2(t)$ and $Q_2(t)$ enter the carrier phase detector unit and complete the acquisition of phase error.

$$\frac{Q_2(t)}{I_2(t)} = \frac{A_1 sin[\Delta\omega t + \Delta\theta]}{A_1 cos[\Delta\omega t + \Delta\theta]} = tan\,[\Delta\omega t + \Delta\theta] \tag{3.79}$$

and

$$\Delta\emptyset = arctan\frac{Q_2(t)}{I_2(t)} = \Delta\omega t + \Delta\theta \tag{3.80}$$

Assuming the satellite ground control station being modelled is a linear system and taking

$$y = \tan[\Delta\omega t + \Delta\theta], z = \frac{dy}{dt} = \Delta\omega sec^2[\Delta\omega t + \Delta\theta] \tag{3.81}$$

and

$$\frac{dz}{dt} = 2\Delta\omega^2 sec[\Delta\omega t + \Delta\theta]y \tag{3.82}$$

then $Eq.$ (3.79) can be modelled as follows using differential equations

$$\frac{Q_2(t)}{I_2(t)} = \frac{1}{2\Delta\omega^2 sec[\Delta\omega t + \Delta\theta]}\frac{dz}{dt}, \qquad \frac{dz}{dt} = \frac{Q_2(t)}{I_2(t)}2\Delta\omega^2 sec[\Delta\omega t + \Delta\theta] \tag{3.83}$$

If $\Delta\omega t + \Delta\theta \approx 0$, the output $Q_1(t)$ of quadrature branch only consists of telemetry sub-carrier and ranging tone sub-carrier signal, and no phase error information exist.

3.3.2 Tracking Receiver

To track an object (e.g. satellite), the angle between the object and the antenna or the error voltage related with the angular error must be detected. The angular error will be modulated onto the error channel signal. Figure 3.8 shows angular error. The angular error signal under the double channel monopulse system is given as

$$E(t) = \Delta A cos(\omega_1 t + \emptyset) + \Delta E sin(\omega_1 t + \emptyset) \qquad (3.84)$$

where, ΔA = azimuth error signal and ΔE = elevation error signal [Xu, 2005].

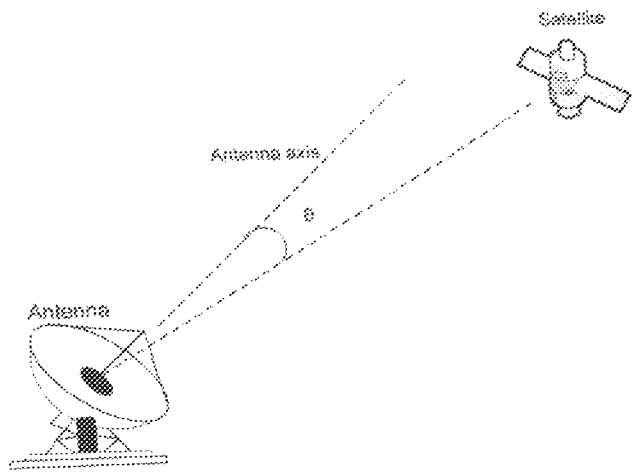

Fig. 3.8 Angular error

In order to get ΔA and ΔE information the phase of input carrier signal must be tracked and then modulated. Figure 3.9 shows the principle of tracking receiver. IF Channel

adjusts the amplitude and filters the noise of the IF signal. Error demodulation unit is made up of quadrature mixer and calibration unit.

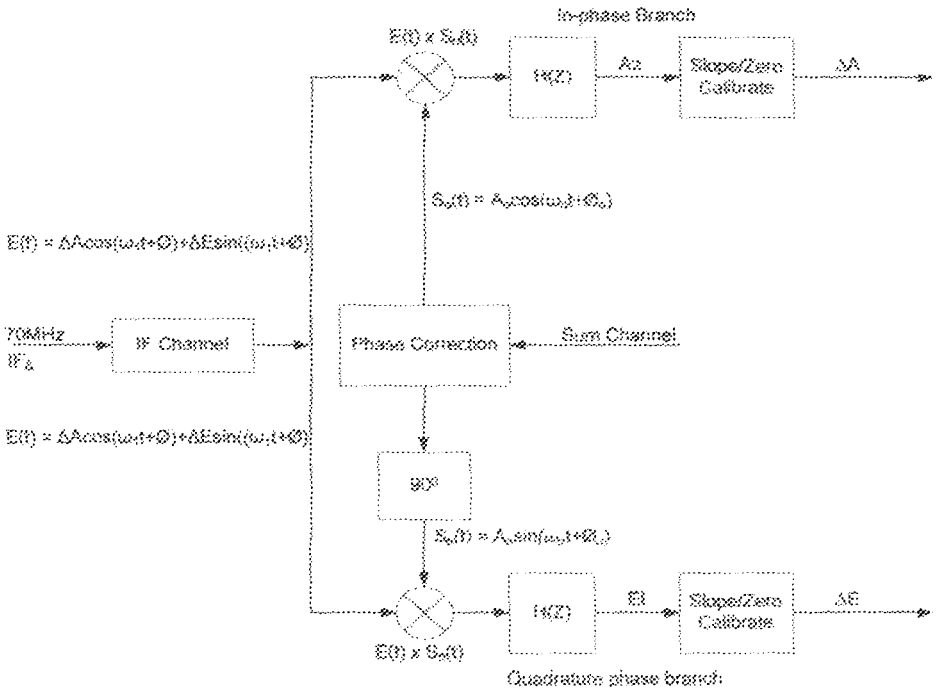

Fig. 3.9: Principle of Tracking Receiver

In-phase branch: It mixes input IF signal (IF_Δ) local signal generated by the in-phase branch ($s_0(t)$) and the local inphase signal generated by the inphase branch. The input IF signal (IF_Δ) is given as (Xu, 2005)

$$IF_\Delta = E(t) = \Delta A cos(\omega_1 t + \emptyset) + \Delta E sin(\omega_1 t + \emptyset) \qquad (3.85)$$

The local in-phase signal generated by the in-phase branch is given as

$$s_0(t) = A_0 \cos(\omega_0 t + \emptyset_0) \qquad (3.86)$$

The mathematical model of the mixture of IF_Δ and $s_0(t)$ is

$$E(t) \cdot s_o(t) = [\Delta A cos(\omega_1 t + \emptyset) + \Delta E sin(\omega_1 t + \emptyset)]x[A_0 \cos(\omega_0 t + \emptyset_0)]$$

$$= \Delta A.\, A_0 cos(\omega_1 t + \emptyset)\cos(\omega_0 t + \emptyset_0) +$$

$$\Delta E A_0 \cos(\omega_0 t + \emptyset_0) sin(\omega_1 t + \emptyset)$$

$$= \frac{\Delta A.\, A_0}{2}\{\cos[(\omega_1 + \omega_0)t + (\emptyset + \emptyset_0)]\} +$$

$$\frac{\Delta A.\, A_0}{2}\{\cos[(\omega_1 - \omega_0)t + (\emptyset - \emptyset_0)]$$

$$+\frac{\Delta E.\, A_0}{2}\{\sin[(\omega_1 + \omega_0)t + (\emptyset + \emptyset_0)]\} +$$

$$\frac{\Delta E.\, A_0}{2}\{\sin[(\omega_1 - \omega_0)t + (\emptyset - \emptyset_0)]\} \qquad (3.87)$$

The low-pass filter removes the sum item and produced the signal

$$E(t) \cdot s_o(t) = \frac{\Delta A.\, A_0}{2}\cos[\Delta\omega t + \Delta\emptyset] + \frac{\Delta E.\, A_0}{2}\sin[\Delta\omega t + \Delta\emptyset] \qquad (3.88)$$

where, $\Delta\emptyset$ = phase offset information between sum and error channel

A_0 = quantizing amplitude of local carrier signature.

Taking $\Delta\omega \cong 0$ (because the baseband signal has a frequency near zero) and eliminating the non-quadrature component we have,

$$E(t) \cdot s_o(t) \cong \frac{\Delta A.\, A_0}{2}\cos[\Delta\emptyset] \qquad (3.89)$$

$$2E(t) \cdot s_o(t) \cong \Delta A.\, A_0 \cos[\Delta\emptyset] = Az \qquad (3.90)$$

Assuming the satellite ground control station being modelled is a linear system and taking

$$y = cos(\Delta\theta), z = \frac{dy}{d(\Delta\theta)} = -\sin(\Delta\theta) \text{ and } \frac{dz}{d(\Delta\theta)} = -cos(\Delta\theta) \qquad (3.91)$$

$Eq.$ (3.90) is modelled as follows using differential equations in $Eq.$ (3.91)

$$Az = -\Delta A A_0 \frac{dz}{d(\Delta\theta)}, \qquad \frac{dz}{d(\Delta\theta)} = -\frac{Az}{\Delta A.\,A_0} \tag{3.92}$$

Quadrature phase branch: It mixes the input IF signal $\{E(t)\}$ and quadrature signal$\{s_0(t)\}$

$$s_0(t) = A_0 \sin(\omega_0 t + \emptyset_0) \tag{3.93}$$

The input IF signal is given as

$$E(t) = \Delta A cos(\omega_1 t + \emptyset) + \Delta E sin(\omega_1 t + \emptyset) \tag{3.94}$$

The mathematical model of the mixture of $s_0(t) and\ E(t)$ by the quadrature mixer is

$$\begin{aligned} E(t)\cdot s_o(t) &= [\Delta A cos(\omega_1 t + \emptyset) + \Delta E sin(\omega_1 t + \emptyset)]\times \\ &\quad [A_0 \sin(\omega_0 t + \emptyset_0)] \\ &= \Delta A.\,A_0 sin(\omega_0 t + \emptyset_0)\cos(\omega_1 t + \emptyset) + \\ &\quad \Delta E.\,A_0 \sin(\omega_0 t + \emptyset_0) sin(\omega_1 t + \emptyset) \\ &= \frac{\Delta A.\,A_0}{2}\{[sin(\omega_0 + \omega_1)t + (\emptyset_0 + \emptyset)] + \\ &\quad [sin(\omega_0 - \omega_1)t + (\emptyset_0 - \emptyset)]\} \\ &\quad + \frac{\Delta E.\,A_0}{2}\{-[cos(\omega_0 + \omega_1)t + (\emptyset_0 + \emptyset)] \\ &\quad + [cos(\omega_1 - \omega_0)t + (\emptyset - \emptyset_0) \end{aligned} \tag{3.95}$$

The low-pass filter removes the sum item and produces the signal

$$E(t)\cdot s_o(t) = \frac{\Delta A.\,A_0}{2}\sin[-\Delta\omega t - \Delta\emptyset] + \frac{\Delta E.\,A_0}{2}\cos[\Delta\omega t + \Delta\emptyset] \tag{3.96}$$

Taking $\Delta\omega \cong 0$ (because the baseband signal has a value near zero) and eliminating the non-quadrature component we have,

$$E(t) \cdot s_o(t) \cong \frac{\Delta E.\mathrm{A}_0}{2}\cos[\Delta\emptyset] \tag{3.97}$$

or

$$2E(t) \cdot s_o(t) \cong \Delta E.\mathrm{A}_0\cos[\Delta\emptyset] = El \tag{3.98}$$

In order to get the exact azimuth and elevation information, the residual phase offset $\Delta\emptyset$ must be eliminated. The automatic calibrate phase is used to get $\Delta\emptyset$.

Assuming the satellite ground control station is a linear system and taking

$$y = cos(\Delta\theta), z = \frac{dy}{d(\Delta\theta)} = -\sin(\Delta\theta) \tag{3.99}$$

and

$$\frac{dz}{d(\Delta\theta)} = -cos(\Delta\theta) = -y \tag{3.100}$$

then *Eqn.* (3.98) can be modelled as follows using differential equations in Eqns. (3.99) and (3.10)

$$El = -\Delta E.\mathrm{A}_0\frac{dz}{d(\Delta\theta)}, \quad or, \quad \frac{dz}{d(\Delta\theta)} = -\frac{El}{\Delta E.\mathrm{A}_0} \tag{3.101}$$

3.3.3 *Telemetry Receiver*

$70\ MHz$ IF signal is received by the telemetry receiver from down converter 1 of Fig. 3.6 and it is expressed as [Xu, 2005]

$$s_k(t) = g(t - kT_s)\cos(\omega_c t + \varphi_k) \tag{3.102}$$

where, φ_k = carrier's phase of the data k, ω_c = angle frequency of carrier

T_s = period of data, $g(t)$ = waveform of the modulated signal's envelope.

Assuming the satellite ground control station is a linear system and taking

$$y = \cos(\omega_c t + \varphi_k), z = \frac{dy}{dt} = -\omega_c \sin(\omega_c t + \varphi_k) \quad (3.103)$$

and

$$\frac{dz}{dt} = -\omega_c{}^2 \cos(\omega_c t + \varphi_k) \quad (3.104)$$

Eqn. (3.102) can be modelled mathematically using *Eqns.* (3.103) and (3.104)

$$s_k(t) = -\frac{g(t - kT_s)}{\omega_c{}^2}\frac{dz}{dt}, \quad or \quad \frac{dz}{dt} = -\frac{s_k(t)\omega_c{}^2}{g(t - kT_s)} \quad (3.105)$$

Telemetry processing unit acquires the clock of sub-carrier signal and performs frame/sub-frame synchronization. Telemetry frames are identified by finding the synchronization word which marks the beginning of the frame in the NRZ-L signal output by the bit synchronizer and in reacting correctly to a loss of lock.

3.3.4 Telecommand Unit

Telecommand unit receives Phase Shift Keying (PSK) modulated telecommand sub-carrier signal expressed as (Xu, 2005)

$$s_k(t) = g(t - kT_s)\cos(\omega_c t + \varphi_k) \quad (3.106)$$

Assuming the satellite ground control station is a linear system and taking

$$y = \cos(\omega_c t + \varphi_k), \; z = \frac{dy}{dt} = -\omega_c \sin(\omega_c t + \varphi_k) \quad (3.107)$$

and $$\frac{dz}{dt} = -\omega_c{}^2 \cos(\omega_c t + \varphi_k) \tag{3.108}$$

Eq. (3.106) can be modelled mathematically using differential equations as follows

$$s_k(t) = -\frac{g(t - kT_s)}{\omega_c{}^2}\frac{dz}{dt}, \quad or \quad \frac{dz}{dt} = -\frac{s_k(t)\omega_c{}^2}{g(t - kT_s)} \tag{3.109}$$

3.3.5 Ranging Unit

The ranging unit processes the ranging tone sub-carrier signal. Tone is a single frequency sin wave signal given as

$$s(t) = A\cos\omega_1 t \tag{3.110}$$

Assuming the satellite ground control station being model is a linear system and taking

$$s(t) = A\cos\omega_1 t,\ z = ds(t)/dt = -A.\omega_1 \sin\omega_1 t \text{ and } dz/dt = -A.\omega_1{}^2 \cos\omega_1 t \tag{3.111}$$

Then, *Eq.* (3.110) can be modelled as follows using *Eq.* (3.111)

$$\frac{dz}{dt} = -A.\omega_1{}^2 \cos\omega_1 t = -A.\omega_1.\omega_1 \cos\omega_1 t, \tag{3.112}$$

then

$$\frac{dz}{dt} = -\omega_1.s(t) \tag{3.113}$$

The distance (S) between the launching and receiving point is given as

$$S = R_0 + R_1 = \frac{\lambda_1 \Delta\varphi}{2\pi} = \Delta\varphi.\frac{c}{2\pi f_1} = \Delta\varphi.\frac{c}{w_1} \tag{3.114}$$

where, R_0 = distance between the satellite ground control station and object

R_1 = distance between the satellite and satellite ground control station

$\Delta\varphi$ = phase delay and λ_1 = wavelength, ω_1 = angular frequency

If the antenna is a transceiver then $R = R_0 = R_1$. Thus,

$$R = \Delta\varphi \cdot \frac{c}{4\pi f_1} \tag{3.115}$$

The higher the tone frequency (f_1), the lesser the ranging error. In baseband system, the frequency group of tones adopted are major tones (27.778kHz) and minor tones (3968Hz, 283Hz, and 35Hz).

3.3.6 IF Modulator Unit

IF modulator performs FM and PM modulation. Its frequency is adjustable between 68 and 72 MHz. The time domain expression of FM (e.g. ranging signal) signal is

$$s_{FM}(t) = A_c \cdot \cos\left[\omega_c t - \int_{-\infty}^{t} k_f Am(\tau)d\tau\right] \tag{3.116}$$

$$= A_c \cdot \cos\ \omega_c t \cdot \cos\left[\int_{-\infty}^{t} k_f Am(\tau)d\tau\right] +$$

$$A_c \cdot \sin\omega_c t \cdot \sin\left[\int_{-\infty}^{t} k_f Am(\tau)d\tau\right] \tag{3.117}$$

Let,

$$I(t) = A_c \cdot \cos\left[\int_{-\infty}^{t} k_f Am(\tau)d\tau\right], Q(t) = A_c \cdot \sin\left[\int_{-\infty}^{t} k_f Am(\tau)d\tau\right] \tag{3.118}$$

The FM signal could be expressed as quadrature vector as follows:

$$s_{PM}(t) = I(t).\cos\omega_c t + Q(t)sin\omega_c t \qquad (3.119)$$

Expression of PM Modulation signal (e g. telemetry and telecommand signal)

$$s_{PM}(t) = \cos\left[\omega_c t - k_p Am(t)\right] = cos\omega_c t.\cos\left[k_p.Am(t)\right] + sin\,\omega_c t.\sin\left[k_p.Am(t)\right] \qquad (3.120)$$

Let,

$$I(t) = \cos\left[k_p.Am(t)\right]\ and\ Q(t) = \sin\left[k_p.Am(t)\right] \qquad (3.121)$$

then,

$$s_{PM}(t) = \cos\left[\omega_c t - k_p Am(t)\right] = I(t).\cos\omega_c t + Q(t)sin\omega_c t \qquad (3.122)$$

3.4 Satellite Control Center (SCC)

SCC simulation system is used for operator trainning, failure handling and backup of the SCC system. This improves SCC system reliability. SCC sends telecommand frames and in return, telemetry and ranging signals are sent to it.

MCS monitors and displays the following information of ground station equipment: operation mode, operation parameters, equipment configuration and status. The system can automatically switch over between the online and the standby equipment, and notify operators for those equipment with redundancy. TFS enables the equipments to be operating at a synchronized time and frequency in the ground station. The overall diagram of satellite ground control station developed is shown in Figure 3.10.

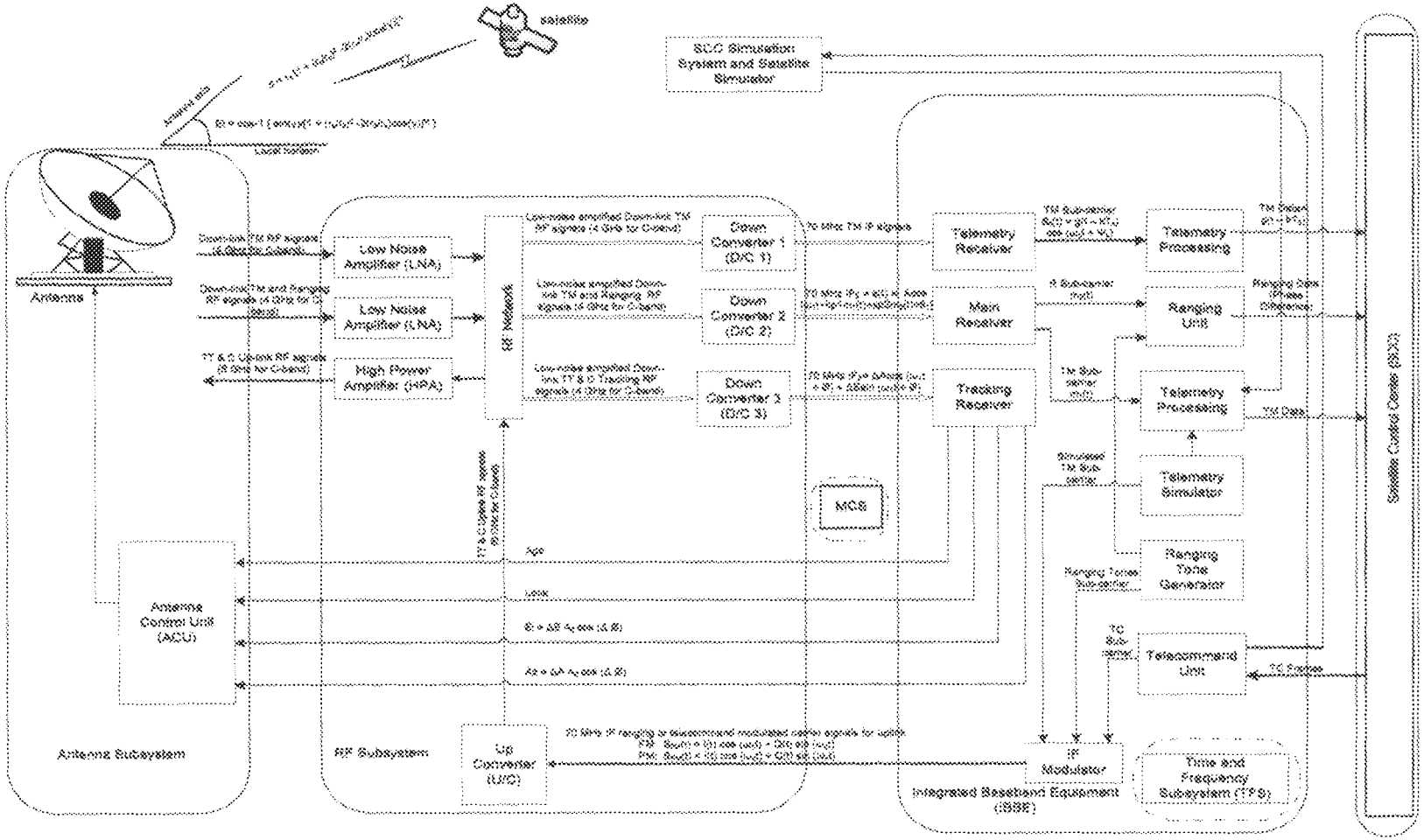

Fig. 3.10 Detailed Drawing of Satellite Ground Control Station

CHAPTER FOUR

4.0 RESULTS

The mathematical equations obtained in Chapter Three were used to carry out the simulation and validation of each of the components of Satellite Ground Control Station modelled. MATLAB software was used to obtain the results shown in the sub-section below, with tables and figures. The explanation of each of the table and figure drawn in this Chapter is given in Chapter Five.

4.1 Range of the Satellite

The MATLAB codes in "*Appendix A*" are used for the validation of the range of the satellite. After the execution of the MATLAB codes, the values generated are shown in Table 4.1.

Figure 4.1 shows the geometry of range and elevation angles calculation showing visible and invisible regions. After the execution of MATLAB codes in *Appendix B*, the plots in Figure 4.2 are obtained.

Table 4.1 Range Validation

S/N	*Gamma, γ, (rad)*	*Range, d, (km)*	*x (km/rad)*	*g (unitless)*
1	0.0000	35786.00	0.00	-1.0000
2	0.1571	35878.40	1172.53	-0.9877
3	0.3142	36151.93	2298.67	-0.9511
4	0.4712	36595.89	3336.11	-0.8910
5	0.6283	37193.51	4249.89	-0.8090
6	0.7854	37923.19	5014.25	-0.7071
7	0.9425	38760.10	5613.05	-0.5878
8	1.0996	39677.52	6038.97	-0.4540
9	1.2566	40648.23	6292.03	-0.3090
10	1.4137	41645.46	6377.91	-0.1564
11	1.5708	42643.66	6306.26	-0.0000
12	1.7279	43619.02	6089.34	0.1564
13	1.8850	44549.80	5740.99	0.3090
14	2.0420	45416.49	5275.86	0.4540
15	2.1991	46201.93	4708.95	0.5878
16	2.3562	46891.31	4055.26	0.7071
17	2.5133	47472.17	3329.71	0.8090
18	2.6704	47934.37	2546.98	0.8910
19	2.8274	48270.09	1721.59	0.9511
20	2.9845	48473.75	867.87	0.9877
21	3.1416	48542.00	0.00	1.0000
22	3.2987	48473.75	-867.87	0.9877
23	3.4558	48270.09	-1721.59	0.9511
24	3.6128	47934.37	-2546.98	0.8910
25	3.7699	47472.17	-3329.71	0.8090
26	3.9270	46891.31	-4055.26	0.7071
27	4.0841	46201.93	-4708.95	0.5878
28	4.2412	45416.49	-5275.86	0.4540
29	4.3982	44549.80	-5740.99	0.3090
30	4.5553	43619.02	-6089.34	0.1564
31	4.7124	42643.66	-6306.26	-0.0000
32	4.8695	41645.46	-6377.91	-0.1564
33	5.0265	40648.23	-6292.03	-0.3090
34	5.1836	39677.52	-6038.97	-0.4540
35	5.3407	38760.10	-5613.05	-0.5878
36	5.4978	37923.19	-5014.25	-0.7071
37	5.6549	37193.51	-4249.89	-0.8090
38	5.8119	36595.89	-3336.11	-0.8910
39	5.9690	36151.93	-2298.67	-0.9511
40	6.1261	35878.40	-1172.53	-0.9877
41	6.2832	35786.00	-0.00	-1.0000

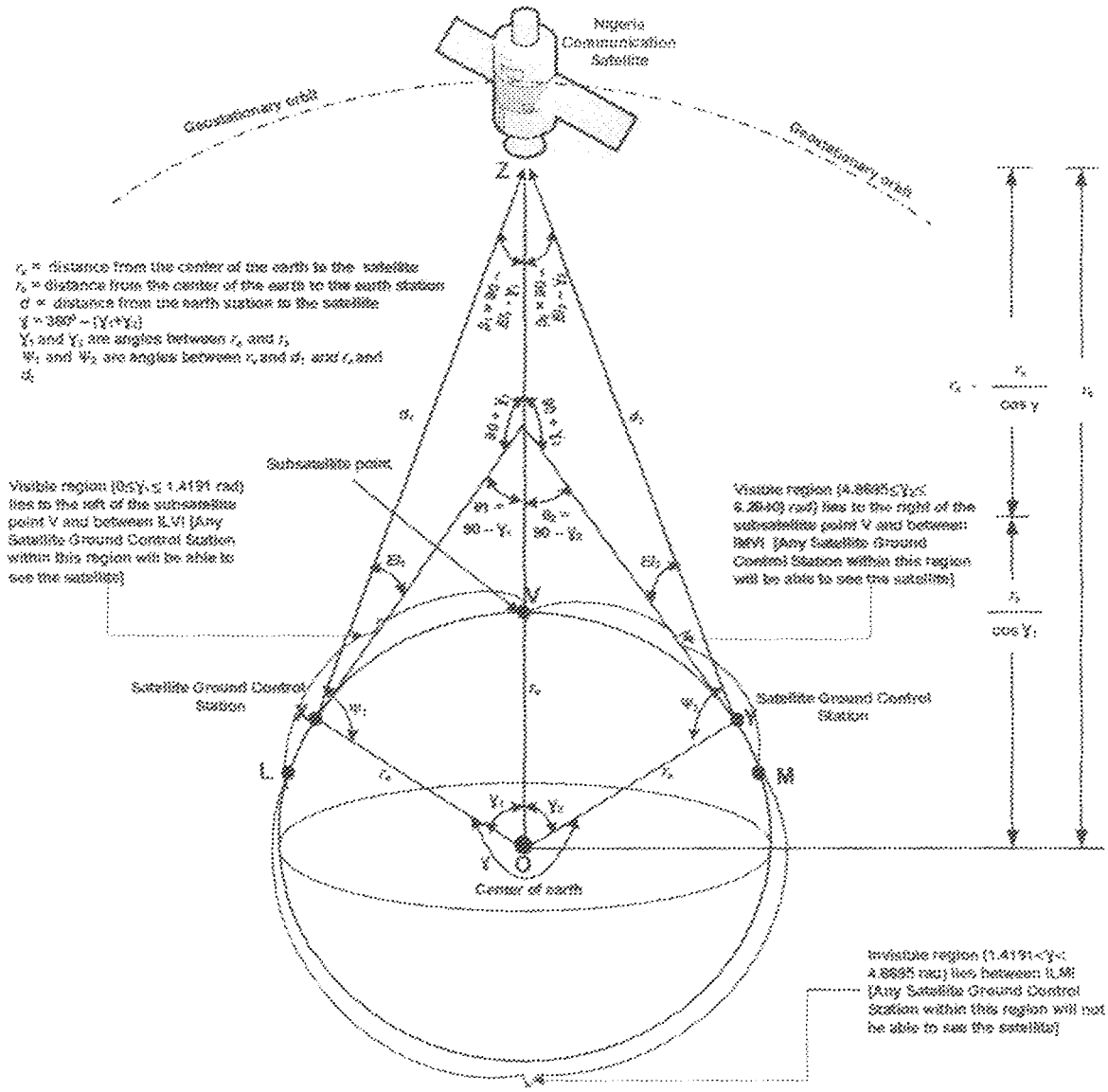

Figure 4.1 Geometry of Range and Elevation angles calculation showing visible and invisible regions

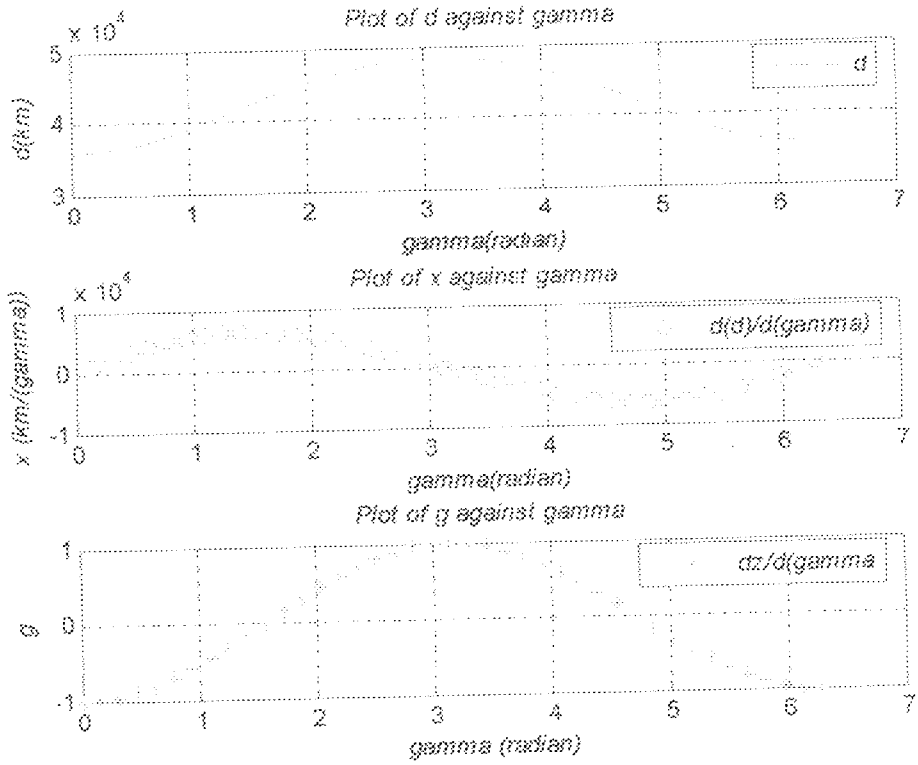

Figure 4.2 Plots of *d* against *gumma*, *x* against *gumma* and *g* against *gumma*

4.2 Elevation Angle of the Satellite

Appendix C lists the MATLAB codes used for the simulation of elevation angle of the satellite. The simulated values are shown in Table 4.2. The plots of elevation angle of Fig. 4.3 are obtained after the execution of the MATLAB codes in *Appendix D*.

Table 4.2 Elevation Angle Validation

S/N	Gamma (radian)	Theta (θ) (radian)	Elevation Angle (radian)	Beta (β) (radian)	q [km/angle]	r
1	0	1.571	1.5708	0.0002	0.0000	1
2	0.1571	1.4139	1.3859	0.0280	-0.0000	0.9877
3	0.3142	1.2568	1.2021	0.0547	-0.0000	0.9511
4	0.4712	1.0998	1.0204	0.0794	-0.0000	0.891
5	0.6283	0.9427	0.8415	0.1012	-0.0000	0.809
6	0.7854	0.7856	0.6662	0.1194	-2.6326	0.7071
7	0.9425	0.6285	0.4948	0.1337	-1.4799	0.5878
8	1.0996	0.4714	0.3275	0.1439	-1.2366	0.454
9	1.2566	0.3144	0.1644	0.1500	-1.1228	0.309
10	1.4137	0.1573	0.0052	0.1521	-1.0524	0.1564
11	1.5708	0.0002	-0.1501	0.1503	-1.0000	0
12	1.7279	-0.1569	-0.3020	0.1451	-0.9548	-0.1564
13	1.8850	-0.314	-0.4507	0.1368	-0.9103	-0.309
14	2.0420	-0.471	-0.5967	0.1257	-0.8619	-0.454
15	2.1991	-0.6281	-0.7402	0.1121	-0.8049	-0.5878
16	2.3562	-0.7852	-0.8817	0.0965	-0.7341	-0.7071
17	2.5133	-0.9423	-1.0215	0.0793	-0.6432	-0.809
18	2.6704	-1.0994	-1.1600	0.0606	-0.5259	-0.891
19	2.8274	-1.2564	-1.2975	0.0410	-0.3773	-0.9511
20	2.9845	-1.4135	-1.4343	0.0208	-0.1983	-0.9877
21	3.1416	-1.5706	-1.5708	0.0002	-0.0000	-1
22	3.2987	-1.7277	-1.4343	-0.2934	0.1983	-0.9877
23	3.4558	-1.8848	-1.2975	-0.5873	0.3773	-0.9511
24	3.6128	-2.0418	-1.1600	-0.8818	0.5259	-0.891
25	3.7699	-2.1989	-1.0215	-1.1774	0.6432	-0.809
26	3.9270	-2.356	-0.8817	-1.4743	0.7341	-0.7071
27	4.0841	-2.5131	-0.7402	-1.7728	0.8049	-0.5878
28	4.2412	-2.6702	-0.5967	-2.0735	0.8619	-0.454
29	4.3982	-2.8272	-0.4507	-2.3765	0.9103	-0.309
30	4.5553	-2.9843	-0.3020	-2.6823	0.9548	-0.1564
31	4.7124	-3.1414	-0.1501	-2.9913	1.0000	0
32	4.8695	-3.2985	0.0052	-3.3037	1.0524	0.1564
33	5.0265	-3.4555	0.1644	-3.6199	1.1228	0.309
34	5.1836	-3.6126	0.3275	-3.9401	1.2366	0.454
35	5.3407	-3.7697	0.4948	-4.2645	1.4799	0.5878
36	5.4978	-3.9268	0.6662	-4.5930	2.6326	0.7071
37	5.6549	-4.0839	0.8415	-4.9254	0.0000	0.809
38	5.8119	-4.2409	1.0204	-5.2613	0.0000	0.891
39	5.9690	-4.398	1.2021	-5.6001	0.0000	0.9511
40	6.1261	-4.5551	1.3859	-5.9410	0.0000	0.9877
41	6.2832	-4.7122	1.5708	-6.2830	0.0000	1

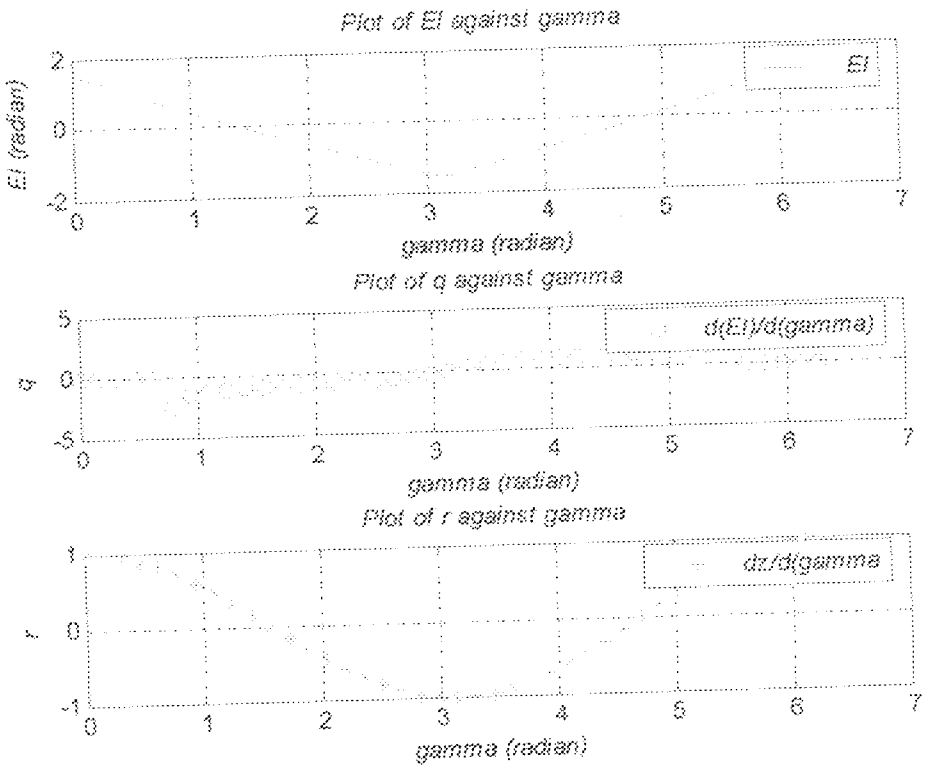

Figure 4.3 Plots of Elevation Angle

4.3 Main Receiver Parameters

The MATLAB codes for the simulation of main receiver parameters is shown in *Appendix F*. The simulated parameters of the main receiver are tabulated in Table 4.3. In Table 4.3, s represents array of change in theta (angle between local horizon and orbital radius), t is the time, a is the frequency, b is the change in angular frequency while p is the linearized value of main receiver and it is dimensionless.

Table 4.3 Main Receiver Simulated Parameters

S/N	*s (radian)*	*t(ms)*	*a (Hz)*	*b (Hz)*	*p*
1	0	220	0	0	0.00E+00
2	0.1571	221	1	6.2832	1.27E+01
3	0.3142	222	2	12.5664	1.08E+02
4	0.4712	223	3	18.8496	4.06E+02
5	0.6283	224	4	25.1327	1.13E+03
6	0.7854	225	5	31.4159	2.79E+03
7	0.9425	226	6	37.6991	6.66E+03
8	1.0996	227	7	43.9823	1.67E+04
9	1.2566	228	8	50.2655	5.03E+04
10	1.4137	229	9	56.5487	2.58E+05
11	1.5708	230	10	62.8319	1.74E+27
12	1.7279	231	11	69.115	3.86E+05
13	1.885	232	12	75.3982	1.13E+05
14	2.042	233	13	81.6814	5.77E+04
15	2.1991	234	14	87.9646	3.62E+04
16	2.3562	235	15	94.2478	2.51E+04
17	2.5133	236	16	100.531	1.82E+04
18	2.6704	237	17	106.8142	1.30E+04
19	2.8274	238	18	113.0973	8.74E+03
20	2.9845	239	19	119.3805	4.57E+03
21	3.1416	240	20	125.6637	9.85E-08
22	3.2987	241	21	131.9469	-5.58E+03
23	3.4558	242	22	138.2301	-1.31E+04
24	3.6128	243	23	144.5133	-2.39E+04
25	3.7699	244	24	150.7964	-4.08E+04
26	3.927	245	25	157.0796	-6.98E+04
27	4.0841	246	26	163.3628	-1.25E+05
28	4.2412	247	27	169.646	-2.49E+05
29	4.3982	248	28	175.9292	-6.17E+05
30	4.5553	249	29	182.2124	-2.68E+06
31	4.7124	250	30	188.4956	-1.00E+27
32	4.8695	251	31	194.7787	-3.06E+06
33	5.0265	252	32	201.0619	-8.05E+05
34	5.1836	253	33	207.3451	-3.72E+05
35	5.3407	254	34	213.6283	-2.14E+05
36	5.4978	255	35	219.9115	-1.37E+05
37	5.6549	256	36	226.1947	-9.19E+04
38	5.8119	257	37	232.4779	-6.18E+04
39	5.969	258	38	238.761	-3.90E+04
40	6.1261	259	39	245.0442	-1.93E+04
41	6.2832	260	40	251.3274	-1.13E-06

The plot of linearization of main receiver of Figure 4.4 is obtained through the running of the MATLAB codes in *Appendix F*.

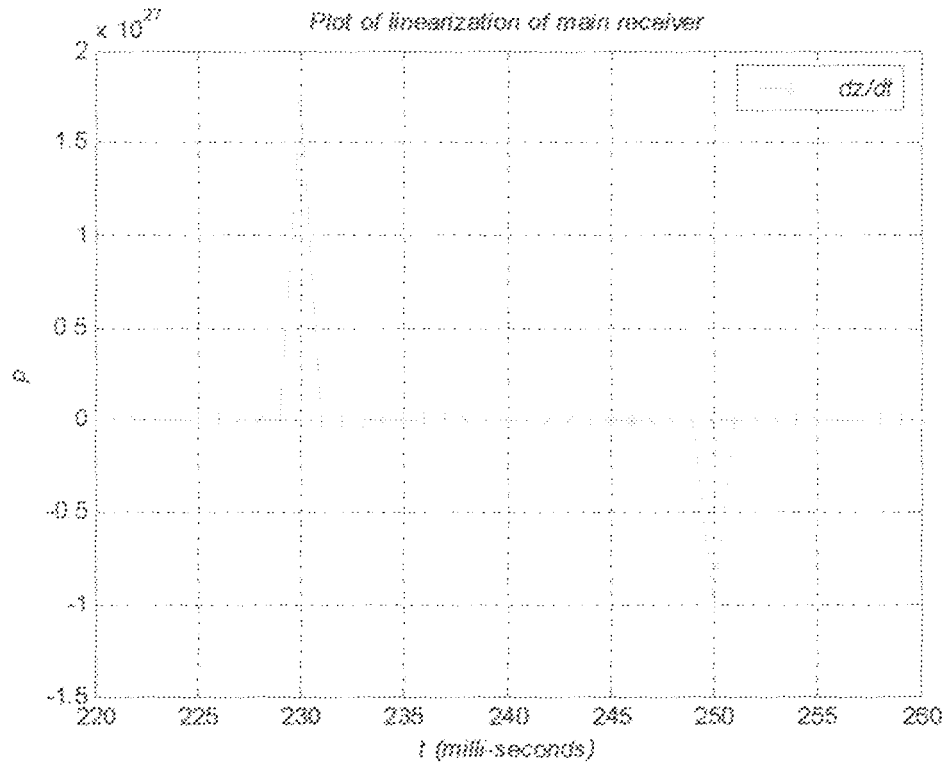

Figure 4.4 Plot of linearization of Main Receiver

4.4 Tracking Receiver Parameters

The simulation of tracking receiver parameters is carried out using the MATLAB codes in *Appendix G* and the simulated data obtained are shown in Table 4.4 and the plots obtained are shown in Figure 4.5.

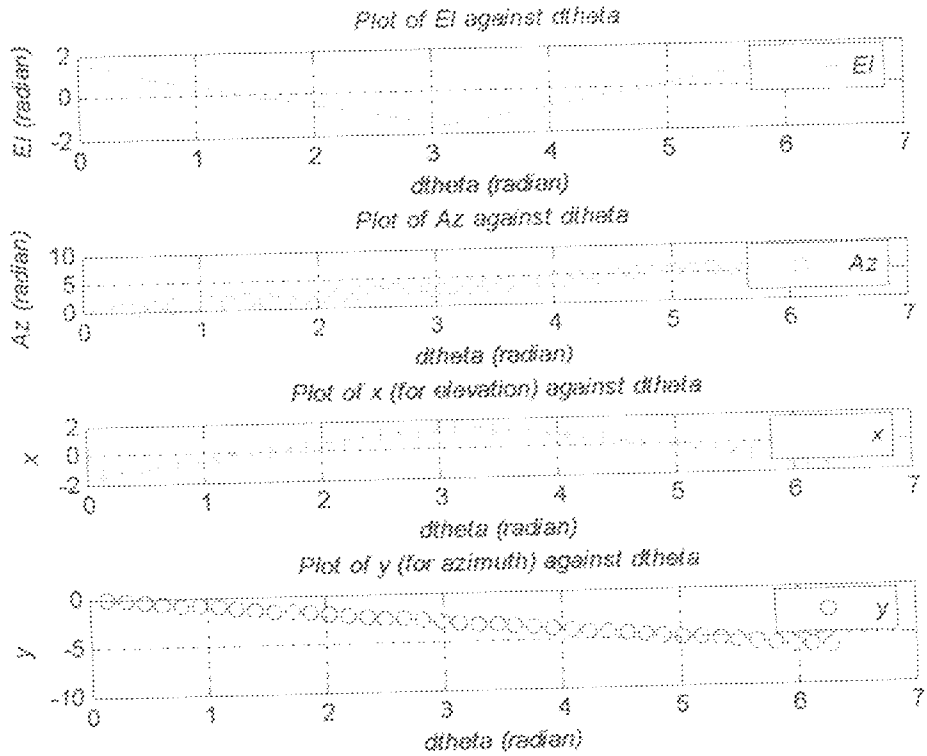

Figure 4.5 Plots of linearization of Tracking Receiver

38	5.8119	1.0204	5.8139	-1.0204	-5.8139
39	5.969	1.7021	5.9690	-1.2021	-5.9690

CHAPTER FIVE

DISCUSSION, CONCLUSIONS AND RECOMMENDATIONS

5.1 Discussions of the Results

Model validation is an essential part of the model development process; hence, if a model is to be accepted and used to support decision making it must be validated. Validation ensures that the model meets its intended requirements in terms of the methods employed and the results obtained. The ultimate goal of model validation is to make the model useful in the sense that the model addresses the right problem and provides accurate information about the system being modelled (Charles, 2005). An unvalidated model is just a hypothesis; as a result, the models of Satellite Ground Control Station developed are validated.

The behaviour of Satellite Ground Control Station models developed are described in two ways: qualitative description and quantitative description. Qualitative description provides an answer to questions about "how", whereas quantitative description answers questions about "how much" (Bender, 1978). In general, qualitative behaviour of satellite ground control station models will be the same for the whole families of models and hence is amenable to general results while quantitative behaviour will be used for the analysis of individual components of the models.

The differential equations used for the linearization of satellite ground control station are written in terms of dimensionless quantities so as to reduce the number of parameters in the equations and make qualitative analysis easier and allow direct comparison of the model types. The results were validated using simulation.

The various aspects of the models of satellite ground control station developed mathematically are simulated as shown in the sections below. Matrix Laboratory (MATLAB) software (Stephen, 2002) was used for the simulation. The analysis in the simulation was carried out using the parameters of Abuja Satellite Ground Control Station and Nigeria Communication Satellite (Nigcomsat-1) as given in Chai (2005). The parameters are as follows:

Satellite longitude (sub-satellite point), $l_s = 42.5^0E$

Satellite latitude, $L_s = 0^0$

Satellite ground control station longitude, $l_e = 7.3891^0$

Satellite ground control station latitude $L_e = 8.9916^0N$

Substituting the values above into Eqns. (3.59), (3.5), (3.15), (3.26) and using radius of the Earth $r_e = 6{,}378.14$ km, and orbital radius $r_s = 42{,}164.17$ km we have,

The central angle, $\gamma_1 = cos^{-1}(\cos(L_e)\cos(l_s - l_e)) = 36.1002^0 = 0.6301 rad$

Range, $d_1 = r_s\left[1 + \left(\frac{r_e}{r_s}\right)^2 - 2\left(\frac{r_e}{r_s}\right)cos\gamma_1\right]^{1/2} = 37{,}201.0110\ km$

Elevation angle, $El_1 = \sin^{-1}\left[\frac{r_s cos\gamma_1 - r_e}{d_1}\right] = 48.1020^0 = 0.8396\ rad$

$$\text{Azimuth angle Az} = A = tan^{-1}\left[\frac{\tan(L_s - L_e)}{\sin(L_e)}\right] = 77.4676^0 = 1.3522\,rad$$

$$B = |L_s - L_e| = |42.5^0 - 7.3891^0| = 35.1109^0\ i.e.\ B > 0,$$

Since $L_e > 0$ *and* $B > 0$, then

$$Az = 180^0 - 77.4676^0 = 102.5324^0 = 1.7898 rad$$

The values obtained above using the mathematical equations developed in Chapter Three will be compared with the values obtained through the validation in order to ascertain the truthfulness and validity of the assumptions made for the models.

5.1.1 Validation of the Range of the Satellite

In carrying out the validation of the range of the satellite Eq. (3.5), Eq. (3.17) and Eq. (3.19) were used. The equations are stated below.

$$d_1 = r_s\left[1 + \left(\frac{r_e}{r_s}\right)^2 - 2\left(\frac{r_e}{r_s}\right)cos\gamma_1\right]^{1/2} \tag{5.1}$$

$$\frac{dz}{d\gamma_1} = \frac{1}{2r_e r_s}\left[{d_1}^2 - {r_s}^2 - {r_e}^2\right] \tag{5.2}$$

$$\frac{d(d_1)}{d\gamma_1} = \frac{r_e x sin\gamma_1}{\left[1 + \left(\frac{r_e}{r_s}\right)^2 - 2\left(\frac{r_e}{r_s}\right)cos\gamma_1\right]^{\frac{1}{2}}} \tag{5.3}$$

In Table 4.1, *gamma*(γ) is the angle between orbital radius, r_s, and radius of the Earth, r_e; range, d, is the distance from the earth station to the satellite; x is the rate of change of range with respect to the central angle (gamma); and g gives the solution of the

differential equation used for the linearization. The unit of x is km/radian and g is unitless because it is dimensionless.

As shown in the Table 4.1 obtained using the MATLAB codes in *Appendix A*, Satellite Ground Control Station X will be able to see the satellite because it lies within the visible region $0 \leq \gamma_1 \leq 81.3^0$ *i.e.* $(0 \leq \gamma_1 \leq 1.4191\, rad)$, which is to the left of the sub-satellite point V shown in Fig. 4.1. Satellite Ground Control Station Y will be able to see the satellite because it lies within the visible region $(4.8695 \leq \gamma_2 \leq 6.2840\, rad)$, which is to the right of the subsatellite point V shown in Fig. 4.1. Abuja Satellite Ground Control Station will be able to see the satellite (Nigeria Communication Satellite) because its central angle $\gamma_1 = 0.6301\, rad$ falls within the visible region $(0 \leq \gamma_1 \leq 1.4191\, rad)$ as indicated in the Table 4.1.

Any Satellite Ground Control Station located within the invisible region, $(1.4191 < \gamma < 4.8695\, rad)$, shaded in Table 4.1 will not be able to see the satellite. Table 4.1 can be used to determine whether a Satellite Ground Control Station lies within the visible region or not using the central angle γ shown in the table.

In the Figure 4.2, "*Plot of d against gamma*" shows the variation of distance (range) with respect to the central angle (gamma). By tracing the value of central angle, gamma (γ_1 *or* γ_2), to the graph in the "*Plot of d against gamma*" the value of the range d of the satellite will be obtained. For example, in the case of Abuja Satellite Ground Control Station with $\gamma_1 = 0.6301\, rad$, the range of Nigeria Communication Satellite is $37{,}200\, km$ after tracing the value of γ_1 to the graph. The value of d obtained is nearly

equal to the calculated value of 37,201.0110 km this shows that the model meets its intended results. The comparison is carried out in order to validate the model.

"$Plot\ of\ g\ against\ gamma$" indicates that at the visible regions $(0 \leq \gamma_1 \leq 1.4191\ rad)$ and $(4.8695 \leq \gamma_2 \leq 6.2840\ rad)$ the system is well linearized because the effects of noise and interference are minimal. However, at the invisible region $(1.4191 < \gamma < 4.8695\ rad)$ there is burge in the curve indicating that there will be a great influence of noise and interference of signals. Therefore it is not advisable to locate a ground station in this region.

5.1.2 Validation of the Elevation Angle of the Satellite

Eqn. (3.15), Eqn. (3.23) and Eqn. (3.24) are used for the validation of elevation angle and they are staied below.

$$El_1 = \sin^{-1}\left[\frac{\left(r_s - \frac{r_e}{\cos\gamma_1}\right)\sin(90+\gamma_1)}{d_1}\right] = \sin^{-1}\left[\frac{(r_s\cos\gamma_1 - r_e)}{d_1}\right] \tag{5.4}$$

$$\frac{dz}{d\gamma_1} = -\frac{1}{r_e}\left[d_1 \sin El_1 + r_e\right] \tag{5.5}$$

$$\frac{d(El_1)}{d(gamma)} = \frac{-r_s x \sin\gamma_1}{(d_1{}^2 - r_s{}^2 x\cos^2\gamma_1 - 2r_e r_s x\cos\gamma_1 - r_e{}^2)^{1/2}} \tag{5.6}$$

In the Table 4.2, $gamma$ is the angle between orbital radius r_s and Earth`s radius r_e, θ is the angle between local horizon and orbital radius, El is the elevation angle, $beta$ is the angle between d (distance from the earth station to the satellite) and orbital radius, q is

the rate of change of elevation angle with respect to the central angle, and r is the linearized value of elevation angle which is dimensionless.

As shown in the Table 4.2, between the visible region ($0 \leq \gamma_1 \leq 1.4191\ rad$), Satellite Ground Control Station X's elevation angles ranges from $1.5708\ rad\ to\ 0.0052\ rad$ and the angles are positive, meaning that it is visible region. Between the visible region ($4.8695 \leq \gamma_2 \leq 6.2840\ rad$), Satellite Ground Control Station Y's elevation angles ranges from $0.0052\ rad\ to\ 1.5708\ rad$ and it is positive, meaning that it is visible region.

In the invisible region ($1.4191 < \gamma < 4.8695\ rad$) shaded in Table 4.2 the elevation angles are negative, indicating that any ground station located in this region will not be able to see the satellite. Since for a nominal geostationary orbit (Timothy *et al.*, 2003) the central angle $\gamma \leq 81.3^0$ ($i.e. \gamma \leq 1.4191\ rad$) and the central angle of Abuja Satellite Ground Control Station used as case study is less than $1.4191\ rad$ ($i.e. \gamma < 1.4191\ rad$), then Nigcomsat-1 is visible to it. Also from the assumption made in chapter three, since $\theta = 90 - \gamma = 90^0 - 36.1002^0 = 53.90^0 = 0.9409\ rad$ lies within the range of ($8.70^0 \leq \theta_1 \leq 90^0$) i.e. ($0.1591 \leq \theta_1 \leq 1.571\ rad$) then the satellite is also visible. Therefore, the proposition is correct and valid.

In Figure 4.3, using *"Plot of El against gamma"* and tracing the central angle ($gamma$) of Abuja Satellite Ground Control Station ($0.6301\ rad$) to the curve, elevation angle of $0.8395\ rad$ was obtained which is very close to the calculated value of

0.8396 *rad*. The comparison shows that the modelled system is in-line with the simulation and well validated. With the negative values of elevation angles, the ground station will not be able to see the satellite.

As seen in the "*Plot of q against gamma*" of Figure 4.3 the rate of change of elevation angle with respect to the angle gamma is nearly uniform due to the linearization of the system. In the Fig. 4.3, the "*Plot of r against gamma*" indicates that the linearized values lie between 1 *and* − 1. When the elevation angles are positive (visible region) the linearized values are also positive; but, when the elevation angles are negative (invisible region) the elevation angles are also negative. The satellite will be visible from the ground station when the elevation angles are positive with positive linearization value and invisible from the ground station when the elevation angles are negative with negative linearization values.

5.1.3 Validation of the Azimuth Angle of the Satellite

Validation of the azimuth angle of the satellite is carried out using Eqns. (3.26), (3.27) and (3.30). The equations are expressed below.

$$\tan A = \frac{\tan|l_s - l_e|}{\sin(L_e)}, \text{ then } A = tan^{-1}\left[\frac{\tan|l_s - l_e|}{\sin(L_e)}\right] \tag{5.7}$$

$$\frac{dA}{dL_e} = -\frac{\cos(L_e).\tan|l_s - l_e|}{\sin^2 L_e + \tan^2|l_s - l_e|} \tag{5.8}$$

$$\frac{dz}{dL_e} = -\tan A \tan|l_s - l_e| \tag{5.9}$$

By running the MATLAB codes in *Appendix E*, the program requests for the values of ls, le and Le from the user. The following values of Abuja Ground Control Station and Nigeria Communication Satellite (Nigcomsat – 1) as given in (Chai, 2005) are used for the simulation; $l_s = 0.7419\,rad$, $l_e = 0.1290\,rad$ and $L_e = 0.1569$. l_s is the longitude of the satellite, l_e is the longitude of the ground station and L_e is the latitude of the ground station. The results obtained at the command prompt are shown as

Enter the value of ls: 0.7419

Enter the value of le: 0.1290

Enter the value of Le: 0.1569

gamma = 0.6302

B = 0.6129

A = 1.3522

k = 3.1650

s = -27.9539

Az = 1.7894

$Az1$ = 31.0955

B is the absolute value of $l_s - l_e$, k is the value of the differential equation (for the linearization), s is the rate of change of angle A with respect to L_e (ground station latitude), Az is the azimuth angle and $Az1$ is the rate of change of azimuth angle with respect to the ground station latitude angle (L_e). The value obtained for the azimuth angle of the ground station, $Az = 1.7894\,rad$, is approximately equal to the calculated value

of $Az = 1.7898\,rad$. This implies that the simulation is conforms with the mathematical model.

5.1.4 Validation of the Main Receiver Parameters

Eqn. (3.83) is used for the validation of main receiver parameters. The equation is

$$\frac{dz}{dt} = \frac{Q_2(t)}{I_2(t)} 2\Delta\omega^2 sec[\Delta\omega t + \Delta\theta] \tag{5.10}$$

As seen in the Table 4.3, the satellite will be visible to the Satellite Ground Control Station between regions $(0\,rad$ and $1.4137\,rad)$ and $(4.8695\,rad\ and\ 6.2832\,rad)$ and the linearized values of the main receiver are very close to zero indicating that the system is very stable and noise and interference have little or no effect on it. In these regions the system is well linearized with values very close to zero.

Between $t = 229\,ms$ and $t = 231\,ms$ shaded in Table 4.3 there is transition from visible region to the invisible region. In this region, there is a very large value of linearization indicating that the system is not stable in this region. Likewise, between $t = 249\,ms$ and $t = 251\,ms$ shaded in Table 4.3 there is also large value of linearization indicating that the system is not stable at this region.

As shown in Figure 4.4, at the transition periods $t = 230\,ms\ and\ t = 250\,ms$, there are high values of linearization of main receiver showing that the system will be unstable at these points. Also at these points, noise and interference will have effect on the system.

5.1.5 Validation of the Tracking Receiver Parameters

The validation of tracking receiver parameters are carried out using Eqns. (3.92) and (3.101). The equations were given as

$$\frac{dz}{d(\Delta\theta)} = -\frac{Az}{\Delta A.\mathrm{A}_0} \tag{5.11}$$

$$\frac{dz}{d(\Delta\theta)} = -\frac{El}{\Delta E.\mathrm{A}_0} \tag{5.12}$$

As shown in Figure 4.5, the *"Plot of x (for elevation) against dtheta"* and the *"Plot of y (for azimuth) against dtheta"* are close to a linear graph. This indicates that all the environmental effects and signal interference on the Satellite Ground Control Station are greatly reduced, and the output signal is a perfect replica of the input signal

In the Table 4.4, $dtheta$ is the change in angle theta (angle between local horizon and orbital radius r_s), El is the elevation angle, Az is the azimuth angle, x is the linearized value of the elevation angle while y is the linearized value of azimuth angle. x and y are dimensionless quantities. The linearized values of the elevation angle, x, and the linearized values of the azimuth angle, y, are very close to zero, indicating that the system is well linearized and the effects of noise and interference on the system are minimal. The invisible region is shaded in the Table 4.4.

5.1.6 Validation of the Ranging Unit Parameters

For the validation of ranging unit Eqns. (3.112)*and* (3.115) are used. The equations are as follows:

$$\frac{dz}{dt} = -A.w_1^2 cosw_1 t \tag{5.13}$$

$$R = \Delta\varphi.\frac{c}{4\pi f_t} \tag{5.14}$$

In Table 4.5, t is the time, f is the frequency, A is the amplitude of the signal, n is the linearized value of the ranging unit and R is the range. As in Table 4.5, the ranging unit is well stable between $t = 0\,ms$ and $t = 129.5500\,ms$ because the system is at ground state and the station has not yet started tracking the satellite. However, there is variation in the linearization of the ranging unit between $t = 136.3500\,ms$ and $t = 272.3500\,ms$ shaded in the table indicating that the ranging unit is slighly unstable because the Satellite Ground Control Station is trying to track the satellite in order to execute the control of the satellite.

As shown in Figure 4.6, the instability in the system is very high between 230 ms and 250 ms because this is the time that the ground station gets hold of the geostationary satellite (Nigcomsat – 1) and then tracks it. The instability could have been caused by the antenna noise, attenuation of the signal and interference. The linearization technique helps to minimize these effects.

5.1.7 Difference Between Real Values and Simulated Values of Abuja Satellite Ground Control Station

As shown in Table 4.6, the percentage difference of range, elevation angle and azimuth angle are very small indicating that the modelled Satellite Ground Control Station is very accurate and close to the real value.

The modelled and validated ground control station gave a detailed description and mathematical representation of the system. The system is an effective training tool which will give the Satellite Ground Control Station (GCS) operator the experience necessary to handle and operate it effectively. In addition, it can be used to learn and practise normal and emergency procedures.

5.2 Conclusions

The models of Satellite Ground Control Station developed were examined using two approaches: qualitative and quantitative. For the whole family of the models, qualitative analysis was used while quantitative analysis was used for the individual components of the models.

Linearization technique was used for the qualitative analysis and the results obtained show that at the visible regions ($0 \leq \gamma_1 \leq 1.4191\, rad$) and ($4.8695 \leq \gamma_2 \leq 6.2840\, rad$) unshaded in the Table 4.1, the system was well linearized because the effects of noise and interference are minimal but at the invisible region ($1.4191 < \gamma < 4.8695\, rad$) shaded in the Table 4.1, the system was not well linearized due to the

influence of noise and interference of signals. It is not advisable to locate a Satellite Ground Control Station in the invisible region. Individual components of the models were tested using quantitative analysis and the results obtained through the validation show that the calculated values were in conformity with the simulated values.

The differential equations used for the linearization were made dimensionless in order to minimize the number of parameters in the equations and make qualitative analysis easier and allow direct comparison of the models. The results were validated using simulation. Through the simulation it was discovered that effects of noise and interference on the system modelled were minimal as shown by the linearization of Figure 4.2 and Figure 4.3.

Abuja Satellite Ground Control Station and Nigcomsat-1 were used for the case study. The values obtained using the mathematical equations developed were compared with the values obtained through simulation in order to verify the assumptions made for the models. The values were in conformity indicating that the modelled equations are right and valid. Nigcomsat-1 satellite was visible from the Abuja Satellite Ground Control Station because the station lies within the visible region.

From the assumption made, since the angle between the local horizon of Abuja Satellite Ground Control Station and orbital radius i.e $\theta_1 = 0.9409\,rad$ lies within the range of $(0.1591 \leq \theta_1 \leq 1.571\,rad)$ then the Nigeria Communication Satellite (Nigcomsat-1) is visible from the ground station. Therefore, the proposition is correct and valid.

5.3 Recommendations

As much work has been done in this thesis as was possible based on the given conditions. However, there are still a number of things that need to be done. The following are the recommendations for future work:

(a) Reliability

In the further work of Satellite Ground Control Station, more elaborate work should be done on the reliability component of the system.

(b) Security

The security of Satellite Ground Control Station is of great importance because of the significance of the data being handled. It is therefore necessary to safeguard these data from being eaveasdropped or tapped by an unknown person. Tight secrurity must be ensured so as to deny untrusted users from accessing the Satellite Ground Control Station network. Therefore, endeavour should be made in the future work to design a secured network for the station.

APPENDICES

MATLAB Codes for the simulation of Various Aspects of Satellite Ground Control Station.

Appendix A: MATLAB Codes for the Simulation of the Range of the Satellite

```
% Script file: Range Simulation
%
% Purpose:
%     To simulate the range of a satellite
%     and save the result.
%
% Record of revisions:
%       Date      Programmer        Description of change
%       ====      ==========        =====================
%     [illegible]  [illegible]      Original Code
%
% Define variables:
%     Number  -- array of number
%     gamma   -- angle between rs and re (radian)
%     rs      -- vector from the center of the earth to the satellite (km)
%     re      -- vector from the center of the earth to the earth station
%                (km)
%     z1      -- cosine of angle gamma
%     z2      -- sine of angle gamma
%     d       -- vector from the earth station to the satellite(km)
%     x       -- rate of change of range with respect to the central
%                angle (d(d)/d(gamma)) (km/radian)
%     g       -- differential equation dx/d(gamma) (for the investigation)
%

% Clear screen
clc;

% Insert an array of number
Number = 1:1:41;

% Create an array of gamma
gamma = 0*pi:pi/20:2*pi;

rs = 42164;
re = 6378;

% Calculate the cosine of angle gamma
z1 = cos (gamma);
```

```
% Calculate the sine of angle gamma
z2 = sin (gamma);

% Calculate the value of length d
d  = rs * ([1+((re/rs).^2)-2 * (re/rs) * z1].^(1/2));

% Calculate the rate of change of range wrt the earth angle
% wrt [d(d)/d(gamma)]
x  = (re * z2) /([1+((re/rs).^2) - 2 * (re/rs) * z1].^(1/2));

% Calculate the differential equation d2d/dgamma2
g  = (d.^2 - rs.^2 - re.^2)/(2*re*rs);

% Display results
fprintf('Number = %5.0f\n', Number);
fprintf('gamma = %6.4f\n', gamma);
fprintf('d = %8.2f\n', d);
fprintf('x = %8.2f\n', x);
fprintf('g = %8.4f\n', g);
```

Appendix B: MATLAB Codes for the Plot of the Graph of Range

```
% This module calculates the value of range (d) in km and plot
% the graph

% Define variables
%       Number -- order of number
%       gamma  -- angle between rs and re (radian)
%       rs     -- distance from the center of the earth to the satellite (km)
%       re     -- distance from the center of the earth to the earth station
%                 (km)
%       z1     -- intermediate variable for the cosine function
%       z2     -- intermediate variable for the sine function
%       d      -- length of range with respect to the centre
%                 angle (d=d(gamma)) (km/radian)
%       g      -- differential equation of gamma wrt the range (d)

gamma = 0*pi:pi/20:2*pi;
rs = 42164;
re = 6378;
d  = rs * ([1+((re/rs).^2)-2 * (re/rs) * cos(gamma)].^(1/2));
x  = (re * sin(gamma)) /([1+((re/rs).^2) - 2 * (re/rs) * cos(gamma)].^(1/2));
g  = (d.^2 - rs.^2 - re.^2)/(2*re*rs);

% Create subplots
subplot(3,1,1)
plot (gamma, d, '--');
title('\fiPlot of d against gamma');
xlabel ('\itgamma(radian)');
ylabel ('\itd(km)');
legend ('\itd');
grid on;
```

```
subplot(3,1,2)
plot (gamma, x, 'bo');
title('\itPlot of x against gamma');
xlabel ('\itgamma(radian)');
ylabel ('\itx (km/gamma))');
legend ('\itd(d)/d(gamma)');
grid on;

subplot(3,1,3)
plot (gamma, g, 'm*');
title('\itPlot of g against gamma');
xlabel ('\itgamma (radian)');
ylabel ('\itg');
legend ('\itdz/d(gamma)');
grid on;
```

Appendix C: MATLAB Codes for the Simulation of the Elevation Angle of the Satellite

```
%   Script file:   Elevation Angle Simulation
%
%   Purpose:
%       To simulate the elevation angle and save the result
%
%   Record of revisions:
%         Date      Programmer        Description of change
%         ====      ==========        =====================
%       20/05/xx   O.A. Ogunbote     Original Code
%
%   Define variables:
%       gamma   -- angle between rs and re (radian)
%       z1      -- cosine of angle gamma
%       z2      -- sine of angle gamma
%       rs      -- vector from the center of the earth to the satellite (km)
%       re      -- vector from the center of the earth to the earth station
%                  (km)
%       theta   -- angle between local horizon and orbital radius (radian)
%       m       -- value of [illegible]
%       El      -- value of elevation angle (radian)
%       beta    -- angle between d and orbital radius rs (radian)
%       q       -- rate of change of elevation angle wrt the orbital angle
%                  gamma i.e. [d(El)/d(gamma)]
%       r       -- the linearized value of elevation angle
%       d       -- the range

 % Clear screen
clc;
```

```
% Create an array of gamma
gamma = 0*pi:pi/20:2*pi;

% Calculate the cosine of angle gamma
z1 = cos (gamma);

% Calculate the sine of angle gamma
z2 = sin (gamma);

rs = 42164.17;
re = 6378.14;

% Calculate angle theta
theta = 1.571 - gamma;

% Calculate the value of m
m  =  (rs*z1)-re;

% Calculate the value of range
d  = rs * ([1+((re/rs).^2)-2 * (re/rs) * cos(gamma)].^(1/2));

% Calculate the value of elevation (El)
El = asin (m./d);

% Calculate angle beta
beta = 1.571 - El - gamma;

% Calculate the rate of change of elevation angle with the need angle
% gamma i.e. [d(El)/d(gamma)]
q  = -(rs * z2)./([d.^2 - (rs.^2)*(z1.^2) - 2 * re*rs*z1 - re.^2].^(1/2));

% Calculate the differential equation r = d(t)/d(gamma)
r  = (d.*sin(El)+ re)./rs;

% Display results
fprintf('gamma = %8.4f\n', gamma);
fprintf('theta = %8.4f\n', theta);
fprintf('El = %8.4f\n', El);
fprintf('beta = %8.4f\n', beta);
fprintf('q = %8.4f\n', q);
fprintf('r = %8.4f\n', r);
```

Appendix D: MATLAB Codes for the Plot of Elevation Angle of the Satellite

```
% This m-file calculates the value of elevation and plot
% the graph

% Define variables
%       gamma  -- angle between rs and re (radian)
%       z1     -- cosine of angle gamma
%       z2     -- sine of angle gamma
%       rs     -- distance from the centre of the earth to the satellite (km)
```

```
%      re     -- distance from the center of the earth to the earth station
%                (km)
%      m      -- value of m/d line
%      El     -- value of elevation angle (radian)
%      q      -- rate of change of elevation angle wrt the central angle
%                gamma i.e. [d(El)/d(gamma)]
%      r      -- the linearized value of elevation angle
%      d      -- the range

gamma = 0*pi:pi/20:2*pi;
rs = 42164;
re = 6378;
z1 = cos (gamma);
z2 = sin (gamma);
d  = rs * ([1+((re/rs) ^2)-2 * (re/rs) * cos(gamma)].^(1/2));
m  =  rs*z1-re;
El = asin (m./d);
q  = -(rs * z2)./([d.^2 - (rs.^2)*(z1.^2) - 2 * re*rs*z1 - re.^2].^(1/2));
r  = (d.*sin(El)+ re)./rs;

%   Create sub plots
subplot(3,1,1)
plot (gamma, El, 'r--');
title('\itPlot of El against gamma');
xlabel ('\itgamma (radian)');
ylabel ('\itEl (radian)');
legend ('\itEl');
grid on;

subplot(3,1,2)
plot (gamma, q, 'bo');
title('\itPlot of q against gamma');
xlabel ('\itgamma (radian)');
ylabel ('\itq');
legend ('\itd(El)/d(gamma)');
grid on;

subplot(3,1,3)
plot (gamma, r, 'm*');
title('\itPlot of r against gamma');
xlabel ('\itgamma (radian)');
ylabel ('\itr');
legend ('\itdr/d(gamma)');
grid on;
```

Appendix E: MATLAB Codes for the Validation of Azimuth Angle of the Satellite

```
%   Script file:   Azimuth angle validation
%
%   Purpose:
%      To validate the azimuth angle and save the results
%
```

```
% Record of revisions:
%      Date       Programmer          Description of change
%      ====       ==========          =====================
%      [illegible]   D.A. Ogundele       Original Code
%
% Define variables:
%   ls        --    longitude of sub-satellite point
%   le        --    longitude of the earth station
%   Le        --    latitude of the earth station
%   gamma     --    angle between ...
%   B         --    absolute value of ls - le
%   A         --    angle A in radians
%   Az        --    azimuth angle (radians)
%   Az1             rate of change of azimuth angle with respect to the
%                   ground station latitude angle (Le)
%   k         --    value of the differential equation dAz/dLe
%   s         --    rate of change of A with respect to Le (dA/dLe)

% Clear screen
clc;

% Prompt the user for the value of longitude of sub-satellite point
ls = input('Enter the value of ls: ');

% Prompt the user for the value of longitude of earth station
le = input('Enter the value of le: ');

% Prompt the user for the value of latitude of the earth station
Le = input('Enter the value of Le: ');

% Calculate the value of the central angle gamma in radians
gamma = acos (cos(Le)*cos(ls - le));

% Calculate angle B
B  = abs(ls - le);

% Calculate angle A
A = atan(tan(B)/sin(Le));

% Calculate the differential equation dAz/dLe
k = - tan(A)*tan(B);

% Calculate the rate of change of A wrt Le (dA/dLe)
s = -tan(B)*cos(Le)/(sin(Le).^2)+(tan(B).^2);

% Calculate the value of azimuth angle
if Le < 0 & B < 0
    Az = A;
elseif Le < 0 & B > 0
    Az = 2*pi - A;
elseif Le > 0 & B < 0
    Az = pi + A;
else
    Az = pi - A;
```

```
end

% [illegible]
if Le < 0 & B < 0
   Az1 = s;
elseif Le < 0 & B > 0
   Az1 = 2*pi - s;
elseif Le > 0 & B < 0
   Az1 = pi + s;
else
   Az1 = pi - s;
end


% Display result
fprintf('gamma = %8.4f\n', gamma);
fprintf('B = %8.4f\n', B);
fprintf('A = %8.4f\n', A);
fprintf('k = %8.4f\n', k);
fprintf('s = %8.4f\n', s);
fprintf('Az = %8.4f\n', Az);
fprintf('Az1 = %8.4f\n', Az1);
```

Appendix F: MATLAB Codes for the Validation of Main Receiver Parameters

```
% Script file: Main receiver validation
%
% Purpose:
%    To validate the linearized values of the main receiver
%    and plot the graph
%
% Record of revisions:
%      Date      Programmer      Description of change
%      ====      ==========      =====================
%      [illegible]      Original Code
%
% Define variables:
%      s    -- array of change in theta
%      t    -- time in millisecond
%      a    -- change in frequency (in Hz)
%      b    -- change in angular frequency
%      y    -- square of angular frequency
%      u    -- value of tan of the function
%      v    -- value of sec of the function
%      c    -- product of u and q
%      p    -- linearized value of the main receiver
% Clear screen
clc;

% Create an array of change in theta (s) in radian
s = 0*pi:pi/20:2*pi.
```

```
% Create an array of time in milliseconds
t = 220:1:260;

% Create an array of change in frequency 'a'
a = 0:1:40;

% Calculate change in angular frequency 'w'
b = 2*pi*a;

% Calculate squares of angular frequency
y = b.^2;

% Calculate the value of tan of the function
u = tan(b.*t + s);

% Calculate the value of sec of the function
q = sec(b.*t + s);

% Calculate product of u and q
e = u .*q;

% Calculate the linear combination of the main receiver
p = 2.*e.*y;

% Display results
fprintf('s = %6.4f\n', s);
fprintf('t = %6.4f\n', t);
fprintf('f = %6.4f\n', a);
fprintf('w = %6.4f\n', b);
fprintf('p = %6.2e\n', p);

% Plot the graph
plot(t, p, 'm--');
xlabel ('\it (milli-seconds)');
ylabel ('\itp');
title('\itPlot of linearization of main receiver');
legend('\itdz/dt');
grid on;
```

Appendix G: MATLAB Codes for the Simulation of Tracking Receiver Parameters

```
% Script file: validation of tracking receiver parameters
%
% Purpose:
%   To validate the linearized values of the tracking receiver
%   and save the result
%
% Record of revisions:
%   Date   Programmer   Description of change
%   ----   ----------   ---------------------
```

```
%     23/05/06  O. A. Ogunsola  --  Original Code
%
%  Define variables
%     dtheta   -- change in theta (radian)
%     gamma   -- angle between rs and re in degrees
%     rs      -- vector from the center of the earth to the satellite (km)
%     re      -- vector from the center of the earth to the earth station
%                in km
%     z       -- cosine of angle gamma
%     d       -- range of the satellite
%     m       -- value of m
%     El      -- elevation angle
%     a       -- absolute azimuth error signal
%     b       -- absolute elevation error signal
%     Ao      -- amplitude of the signal
%     Az      -- azimuth angle of the signal
%     x       -- linearized value of elevation angle
%     y       -- linearized value of azimuth angle
%  Clear screen
clc;

%  Create an array of change in theta in radian
dtheta = 0*pi:pi/20:2*pi;

%  Create an array of gamma
gamma = 0*pi:pi/20:2*pi;

rs = 42164;
re = 6378;

%  Calculate the cosine of angle gamma
z = cos (gamma);

%  Calculate the value of range d
d  = rs * ([1+((re/rs).^2)-2 * (re/rs) * z].^(1/2));

%  Calculate value of m
m  =  rs*z-re;

%  Calculate the value of elevation (El)
El = asin (m./d);

%  Create an array of absolute azimuth error signal
a = 0:1:40;

%  Create an array of absolute elevation error signal
b = 0:1:40;

%  Create an array for the amplitude of the signal
Ao = 0:1:40;

%  Create an array for the azimuth angle of the signal
Az = 0*pi:pi/20:2*pi;
```

```
% Calculate the horizontal offset of tracking receiver
x = -(El)./b.*Ao
y = -(Az)./a.*Ao

% Display results
fprintf('dtheta = %8.4f\n', dtheta);
fprintf('El = %8.4f\n', El);
fprintf('Az = %8.4f\n', Az);
fprintf('x = %8.4f\n', x);
fprintf('y = %8.4f\n', y);

% Create subplots

subplot(4,1,1)
plot (dtheta, El (radian), 'r--');
title('\bfPlot of El against dtheta');
xlabel ('\bfdtheta (radian)');
ylabel ('\bfEl');
legend ('\bfEl');
grid on;

subplot(4,1,2)
plot (dtheta, Az, 'bx');
title('\bfPlot of Az against dtheta');
xlabel ('\bfdtheta (radian)');
ylabel ('\bfAz (radian)');
legend ('\bfAz');
grid on;

subplot(4,1,3)
plot (dtheta, x, 'm*');
title('\bfPlot of x (for elevation) against dtheta');
xlabel ('\bfdtheta (radian)');
ylabel ('\bfx');
legend ('\bfx');
grid on;

subplot(4,1,4)
plot (dtheta, y, 'ko');
title('\bfPlot of y (for azimuth) against dtheta');
xlabel ('\bfdtheta (radian)');
ylabel ('\bfy');
legend ('\bfy');
grid on;
```

Appendix H: MATLAB Codes for the Simulation of Ranging Unit Parameters

```
% Script file: 'Evaluation of Ranging Unit Parameters'
%
% Purpose:
```

```
%     To calculate the ranging parameters
%
% Record of revisions
%      Date     Programmer      Description of change
%      ====     ==========      =====================
%      [illegible]  O.A. Ogundele    Original Code
%
% Define variables:
%      c     -- velocity of light
%      p     -- phase delay
%      t     -- time
%      f     -- frequency
%      A     -- Amplitude of the signal
%      w     -- angular frequency
%      d     -- cosine of the function
%      n     -- linearized value

% Clear screen
clc;

c = 10.8*(10 ^8);

% Create an array of change in phase delay in radian
p = 0*pi:pi/20:2*pi;

% Create an array of time in milli seconds
t = 0.35:6.8:275;

% Create an array of ranging tone frequency (in Hertz)
f = 35:680:27800;

% Create an array of the amplitude of the signal
A = 0.070:1.36:55.0;

% Calculate angular frequency (w)
w =  2*pi*f;

% Calculate the value of cosine of the function
d = cos(w.*t);

% Calculate the linearized value of ranging unit n
n = -A.*d.*(w.^2);

% Calculate the products of change in phase delay and velocity c
s = p.*c;

% Calculate the value of b
b = 4*pi*f;

% Calculate range of the satellite
R = s./b;

% Display results
```

```
fprintf('t = %8.4f\n', t);
fprintf('f = %8.4f\n', f);
fprintf('A = %8.4f\n', A);
fprintf('n = %8.4f\n', n);
fprintf('R = %8.4f\n', R);

%  Create plot

plot (t, n, 'r--');
title('\tPlot of n against time');
xlabel ('\tTime (milli - seconds)');
ylabel ('\tn ');
legend ('\tn, linearized value');
grid on;
```